EMERGING PULSED ELECTRIC FIELD AND OSCILLATING MAGNETIC FIELD COMBINATION TECHNOLOGIES ON FOOD FREEZING

A THESIS SUBMITTED TO THE GRADUATE DIVISION OF THE UNIVERSITY OF HAWAI'I AT MĀNOA IN PARTIAL FULFILLMENT OF THE REQUIREMENTS FOR THE DEGREE OF

MASTER OF SCIENCE

IN

FOOD SCIENCE

DECEMBER 2013

By

Jin Hong Mok

Thesis Committee:

Dr. Soojin Jun, Chairperson

Dr. Alvin Huang

Dr. Yong Li

ACKNOWLEDGEMENTS

I would like to express my deep appreciation and sincere gratitude to the following people for helping me complete this thesis.

Dr. Soojin Jun, my advisor, gives the continuous support, confidence, scientific advice and, especially, for his amazing motivation and implication. As a member of his team, I learned amazing pursue avenues of my research with his valuable insight and scientific breakthroughs. He also fosters an atmosphere of challenges and power of trust and happiness.

My committee members, Dr. Alvin Huang and Dr. Yong Li, were thorough and insightful. They gave me support and expertise throughout the courses of my academic research. I would like to thank Dr. Wayne Iwaoka, Dr. Yong Soo Kim, Dr. Frederic Mercier and Dr. Won Choi for their generous advice and consideration during completion of my research and thesis. I thank all of them for their time, knowledge and instruction during my time at University of Hawaii.

Many thanks to my fellow group members in the food processing lab for sharing their latest breakthroughs and the excitement those discoveries bring. They were always Room #118 with equipment expertise, scientific know-how and great conversation topics.

Finally, I am forever thankful for the love and support of my family. They were always excited to hear about my work and often provided new ways of thinking that led me to the answers I needed.

It has been really great full-two years!

ABSTRACT

Recently, new emerging freezing technologies have been developed to alternate traditional and inefficient freezers. However, due to water crystallization, the consequence of freezing and thawing that can impact on quality of food composition and microstructure remains as critical issues. In present study, combination of pulsed electric field (PEF) and two different types of magnetic fields were applied to resolve the outstanding freezing problems. The concept was that when a polar liquid (i.e. water) is exposed to an external electric field, it would undergo polarization that re-orientates and vibrates water molecules. Also, water is diamagnetic which may develop a magnetic dipole moment in quick response to an applied magnetic field, leading to rearrangement of water molecules. Thus, combination of these two field strengths was hypothesized to effectively interrupt critical ice nucleation in food matrices and extend the supercooling status of foods even at subzero temperatures. As a result, the growth pattern of ice crystals and phase transition time of 0.9% NaCl solution were investigated and compared under individual and combination of PEF (1.78 V/cm, duty cycle: 0.5) and static magnetic field (SMF). The combination effect of PEF at 20 kHz and repulsive SMF treatments at a freezer temperature of -20°C showed an increased number of the finest and round ice crystals (equivalent diameter: 97 ± 12 μm; roundness: 0.90 ± 04; elongation: 1.24 ± 0.33) during the shortest phase transition time (1004 ± 3 sec). The second approach included an innovative maintenance of fresh food qualities (i.e. chicken breasts) by establishing a stable supercooling state by combination of PEF and oscillating magnetic field (OMF). Supercooled chicken breasts preserved at -7°C for 12 hours showed little apparent food tissue damages and the overall degrees of

qualities deterioration (i.e. drip loss, color, texture, pH and lipid oxidation) were significantly lower than control samples in refrigeration and freezing storage. The developed technology will have the potential to ensure food quality and freshness during storage, which would have an enormous impact on food industries.

TABLE OF CONTENTS

CHAPTER 2

CHAPTER 3

LIST OF TABLES

LIST OF FIGURES

LIST OF ABBREVIATIONS & SYMBOLS

A	internal cross-sectional area (m^2)
A	internal cross-sectional area of ice crystal (μm^2)
a^*	redness-greenness
ANOVA	analysis of variance
b^*	yellowness-blueness
BHT	butylated hydroxytoluene
CCD	charge-coupled device
D	duty cycle (θ)
E	electric field strength (V/m)
e	elongation
EF	electric field
HCl	hydrochloric acid
I	electric current (A)
IGBT	integrated-gate-bipolar-transistor
INA	ice nucleation activators
L	distance between two electrodes (m)
L^*	lightness
M	force moment exerted on the dipole
m	slope variable
MDA	malondialdehyde
MF	magnetic field
NaCl	sodium chloride
NdFeB	neodymium permanent disc magnet
OMF	oscillating magnetic field
P	polarization (C/m^2)
p	perimeter (μm)
P-T	pressure-temperature
PE	polyethylene
PEF	pulsed electric field
PEF+repulsive SMF	combination of PEF and repulsive SMF
q	equivalent charge
R	roundness
r	radius of the nuclei sphere (m)
r^*	critical radius size of nuclei sphere (m)
S.D.	standard deviation
SMF	static magnetic field
T	temperature (K)
T_b	boiling point (K)
T_f	freezing temperature (K)
T_g	glass transition point (K)
T_H	homogeneous nucleation point (K)

T_m	melting point (K)
T_{SH}	superheating temperature (K)
T_x	crystallization point (K)
TBA	thiobarbituric acid
TBARS	thiobarbituric acid reactive substances
TCA	trichloroacetic acid
V	applied voltage (V)
$V_{p\text{-}p}$	peak-to-peak voltage ($V_{p\text{-}p}$)
V_m	molar volume (m^3/mol)
gamma	
γ	surface free energy of the crystal fluid interface (J/m^2)
delta	
ΔE	net color difference
ΔG	free energy (J/m^3)
ΔG_E	free energy needed for formation of a spherical nucleus (J/m^3)
ΔG_v	free energy of freezing per unit volume (J/m^3)
$\Delta H_{m,f}$	molar enthalpy of fusion (J/mol)
ΔT_{sc}	degree of supercooling (°C)
mu	
μ_0	dipole moment
sigma	
σ	electrical conductivity (S/m)
σ_{ref}	reference electrical conductivity (S/m)

CHAPTER 1

INTRODUCTION & LITERATURE REVIEW

1.1. Introduction

With the growing accessibility of food markets and broad integration of food supply chains in worldwide, the assurance of food quality has become a major concern. Therefore, most of the changes attributed to food quality have been inspected and minimized under careful management during food storage and supply so that the food available for consumption meets consumer's quality expectation. However, there are still numerous circumstances that can occur where food products are exposed to inappropriate storage conditions, resulting in undesired changes in color, odor, taste and texture. These changes will ultimately lead to an overall deterioration in food quality. A continuation of food quality losses eventually renders the product unacceptable and negative impacts on the loss of economic value of food products directly by wasting the resources used in production such as land, water, energy, and other inputs. In order to minimize the quality losses and changes on the fresh-like characteristics, food preservation techniques have been employed and developed.

Among the various food preservation methods, freezing has been widely used as the most efficient method by transformation from the liquid to solid state of water content of the food. Food freezing has been successfully employed for the long term stability to foods from domestic to industrial scales with a high degree of safety, nutritional value and sensory quality by delaying chemical changes, retarding the enzyme action and eliminating the microbial growth.

Nonetheless, the freezing technology still deals with serious problems in terms of food quality during freezing storage of foods. A major reason is due to the osmotic transfer of water throughout the cell membrane and the growth of extracellular ice crystals, leading to structural damage on food tissue. More specifically, volumetric expansion associated with the water-ice transition leads to internal stress that prevents the structures from relaxing back into its original shape, and mechanical damages on the texture of food tissue. Therefore, the understandings of the ice crystallization process and related phenomena in regard to the crystal characteristics are very essential for the improvement of food freezing processes. This section presents the theoretical backgrounds on freezing mechanisms and the review of recent developments in the freezing technologies and their effects of ice crystallization.

1.2. Literature Review

1.2.1. Freezing as a food preservation

A majority of food products are perishable by nature and, thus, they need to be processed to maintain their qualities during preparation, storage and distribution. In addition, since food products are transferred and consumed in areas of the world far distant from their production sites, promoting longer shelf life and reduced hazard from eating the food are required. For solving this problem, food preservation processes have been investigated and developed.

As representative food preservation methods, thermal process, atmosphere packaging, refrigeration and addition of chemical preservatives compounds can be used to reduce the undesirable chemical changes and risk of outbreaks of food poisoning; however,

these techniques frequently have associated adverse changes in organoleptic characteristics and loss of nutrients. Within this framework, limiting food quality losses due to enzymatic reactions and sensory characteristics, freezing can be an excellent method that can preserve many food products in an acceptable form for consumers close to their original qualities during the extended period.

Freezing is one of food preservation methods that delays the physical, chemical and microbiological activities by reducing the temperature of all parts of the food products below the freezing point. The freezing point varies depending on the concentrations of dissolved substances of food products.

The application of freezing for longer term storage of harvested and prepared foods has been done for thousands of years (Persson and Londahl, 1993). In ancient times, techniques for freezing foods were a necessity that developed from the absolute need to survive in a hostile environment where fresh food was not always available. However, in modern times, freezing was employed to ensure the quality of human diet, minimize food loss and facilitate transportation and distribution (Xanthakis et al., 2013). More recently, the focus has shifted to convenience for consumers and higher quality of much various types of food products. Accordingly, the market for frozen foods has grown by the rate of 2.6% from 2008 to 2013 reaching a value of $28 billion in the US primarily due to demands for faster ready-to-eat foods and new product launches in the market. In addition, there are increasing numbers of consumers expecting a wide variety of foods to be available year-around, but without the preservatives that have made year-round availability attainable. Since the moisture content of food products range between 50 and 95%, existing in different forms in the food tissues, freezing of food products should address the consist of

the transition of the majority of water contained in the food tissues into ice. Recent theoretical and experimental approaches are increasingly directed towards the potentials to control the ice crystallization during freezing in order to extend the original freshness before the use of food products.

1.2.2. Freezing mechanism

During food freezing, a gradual decrease in the product temperature occurs as heat is removed from water within the product. To describe the physical changes of water within the food product, the context of thermodynamics can be applied. In freezing, there are two different heat transfer phenomena: (i) sensible heat which is removed to lower the temperature of product to the freezing point and (ii) latent heat of fusion which is then removed and ice crystals are formed.

At atmospheric pressure, the ice crystallization process can be divided into three subsequent stages. During the first stage of cooling, the temperature falls to just below 0°C, the freezing point of water. As more heat requires to be extracted, temperature of water below its freezing points but water remains liquid without becoming a solid. This phenomenon is known as 'supercooling' (Fig. 1.1). The supercooling state can be maintained and only sensible heat is removed until the nucleation begins. The sudden increase in water temperature reaches the freezing point and ice crystals begin to form with a release of latent heat of fusion. The freezing proceeds into the solidification process at the freezing point continuously. During this freezing period, the ice crystals grow and agglomerate themselves. The growth rate of ice crystal is related with the rate of heat transfer (Hu et al., 2013). After completion of ice crystallization, the ice temperature falls

down to the surrounding temperature as the remaining sensible heat is removed from the ice.

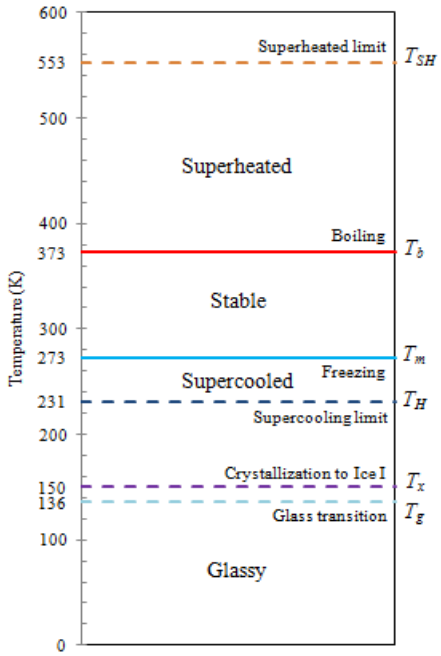

Figure 1.1. Phase of liquid water at atmosphere and temperature range of corresponding phase. T_{SH}: superheating temperature; T_b: boiling point; T_m: melting point; T_H: homogeneous nucleation point; T_x: crystallization point; T_g: glass transition point.

1.2.3. Supercooling of water

Water has more than 16 crystalline phases under different temperature and pressure combinations and displays unique behavior such as supercooling (Bigg, 1953; Stokely et al., 2010). Such anomalous behaviors and structures of water have been intensively studied and, in particular, the properties of supercooled water have been investigated since discovered by Fahrenheit in 1724 (Shaw et. al., 2005). Supercooled water is in a metastable state, and its rapid transition to ice makes it difficult to control the crystallization process.

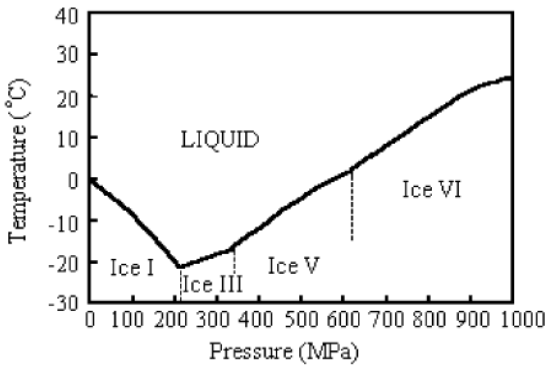

Figure 1.2. Phase diagram of water (Li and Sun, 2002).

During the phase transition of water to more structurally ordered state, which may have lower Gibbs free energy, the less ordered phase can continue to exist (Petrenko and Whitworth, 1999). Several extended lines between two phases in the pressure-temperature (P-T) diagram of water represent the region of liquid state's stability at equilibrium and the metastability can be maintained within the phase equilibrium boundaries (Fig. 1.2). Most of these extended lines are due to the tendency of hydrogen bonds formation between neighboring water molecules. As the cooling process proceeds, the structure of liquid water can change along with decreases of local potential energy and entropy, and an increase in the local volume by the forming of local open structures of bonded molecules (Tanaka, 2000; Stokely et al., 2010). When seeding is introduced, water in supercooling state can turn into ice and various ice crystal structures can be obtained at several pressure levels from atmospheric pressure up to 300 (Otero and Sanz, 2000; Schlüter et al., 2004). The effects of external freezing enhancers such as rubbing, collision, vibration, and shock on the supercooled water have been studied at various levels (Goyer et al., 1964; Kashiwagi et al., 1987; Saito et al., 1992).

In addition, due to stochastic characteristics of the supercooling, freezing transformation is not reproducible even at the same temperature profile, which might be explicable using the conventional theory of nucleation associated with the probability of crystallization in a sample per time (Turnbull, 1956).

1.2.4. Physical properties of water freezing

During a phase transition, thermodynamic properties of substances are changed corresponding to external conditions, such as temperature and pressure. If the perturbation of conditions is not enough to be destabilized, substances stay as metastable. (Tolbert et al., 1995). If the perturbation has grown large enough, then, tiny crystal embryos called nuclei are formed and aggregated. The individual nucleus formation is dependent on the change in Gibbs free energy as a result of its growth or shrinkage. In liquid water, surface free energy increases with the square of crystal size as there is an interfacial tension between the two phases while the free energy of crystallization decreases with the cube of size. The change in overall free energy of crystal formation as a function of crystal nucleus size can be calculated as:

$$\Delta G_E = 4\pi r^2 \gamma - \frac{4}{3}\pi r^3 \Delta G_v \tag{1.1}$$

where r is the radius of the nuclei sphere (m), γ is the surface free energy of the crystal fluid interface (J/m^2), and ΔG_v is the free energy of freezing per unit volume (J/m^3) given by:

$$\Delta G_v = \frac{\Delta H_{m,f}(T_f - T)}{T_f V_m} \tag{1.2}$$

where $\Delta H_{m,f}$ is the molar enthalpy of fusion (J/mol), V_m is the molar volume (m^3/mol), T_f is the freezing temperature, T is the temperature of the investigation, and $T_f - T$ represents the degree of supercooling (ΔT_{sc}). From Equation (1.1), there is a maximum energy preventing the formation of crystals and overcoming that barrier determines the kinetics of nucleation. A lower energy barrier to nucleation implies the time needed for nucleation is lower and the nucleation rate is higher. If the ice embryo is larger than this critical size (r*), it continues to increase up to an ice crystal (Fig. 1.3). The critical size can be expressed as r* given by:

$$r^* = \frac{2\gamma}{\Delta G_v} \tag{1.3}$$

From the Equation (1.3), the degree of supercooling (ΔT_{sc}) can affect to the critical nucleus radius and it would be correlated with ice crystal size.

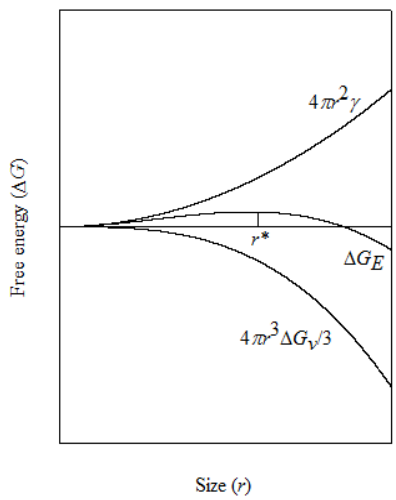

Figure 1.3. Gibbs free energy (ΔG) changes associated with formation of a stable nucleus. r* is the critical size of nuclei.

1.2.5. Current freezing technologies and drawbacks

Food industries are continually making efforts to innovate the freezing technologies that serve products to consumers that are, not only safe, fresh and delicious, but also minimally processed, nutritious, and shelf- and refrigerator-stable. Bringing all these attributes into a food product and keeping the product as inexpensive as possible for the consumers are great challenges for today's food technology industries.

For large-scale variations in the supply and demand for premium quality of food products, a variety of freezing systems have been developed to effectively store food products at the constant low temperature for short time period. Commercial freezers have been designed based on the properties of fresh produce. Although current freezing techniques offer many advantages, a certain degree of degradation in food quality during freezing storage still exists. Most of irreversible damages on food tissues are affected by storage time–temperature conditions and product types.

The undesirable chemical changes and deterioration of nutrient quality include protein insolubilization, lipid oxidation and hydrolysis, natural pigment degradation, vitamin deterioration and brown pigment formation (Fennema, 1977; Canet, 1989; Pilar Cano, 1999; Campañone et al., 2001; Martins and Silva, 2002; Giannakourou and Taoukis, 2003; Gonçalves et al., 2011). In fruits and vegetables, textural changes throughout freezing storage are derived from structural alteration of protein membranes and disruption of cellulosic cell walls due to ice crystal growth (Powrie, 1984). In meat samples, the noticeable color and flavor alteration during the storage due to lipid and myoglobin oxidation and reductions in weight and texture defects are the main adverse changes affecting the quality of frozen red meats (Soyer et al., 2010).

In addition, the physical aspects in consideration include low surface heat transfer (air blast freezer), dilution of solution with product and limitation on regular-shaped materials (contact freezer), and high operating cost (cryogenic freezer) (Barbosa-Cánovas et al., 2005). In order to overcome these technical issues, emerging freezing techniques have been designed and developed.

1.2.6. Emerging technologies for food freezing

The application of ultrasound to liquid freezing has potentials and has been looking promising over the last few years. The ultrasound energy generates physical effects in the receiving medium such as the cavitation phenomenon, causing the formation of gas bubbles. The gas bubbles can serve as nuclei for ice nucleation (Mason et al., 1996) or affect the crystallization by their collapse and motion. Furthermore, the ultrasound influences the initiation of crystal nucleation, the growth rate of crystals, and the formation of small and even-sized crystals (Virone et al., 2006; Luque de Castro and Priego-Capote, 2007). However, more fundamental research is needed in order to identify the most important factors that affect the ability of ultrasound in achieving the desired quality factors. Considerable research efforts are in need for the design, the scale-up and the development of adequate industrial equipment.

High hydrostatic pressure has been known as a new protocol to enhance the freezing process and it has been a subject of research in recent decades (Norton and Sun, 2008; Schlüter et al., 2009). The use of high pressure makes high degrees of supercooling possible, resulting in rapid ice nucleation and growth all over the sample under pressure release. With multi-steps pressure controls, the size and types of ice crystals can be manipulated

for significant improvement of food product quality. However, the limitations of this process include poor stability of operation, less effectiveness in the cooling process under the pressure, protein denaturation induced by high pressure, and different resistance to higher pressure with food nature (Le-Bail et al., 2002).

Ice nucleation activators (INA), which are protein complexes in bacteria's outer membrane, have been applied to catalyze the formation of ice in supercooled water at high subzero temperatures (Zachariassen and Kristiansen, 2000; Zhang et al., 2010). The addition of INA to food samples leads to an increased temperature of ice nucleation, shortened freezing time, and increased freezing rate. The presence of INA bacteria has been highlighted with the potential to improve the quality of solid frozen foods (Zhang et al., 2010). However, the addition of INAs has disadvantages in its safety issues, such as ensuring for non-toxic and non-pathogenic microorganisms and completely killing inedible microorganisms before foods are consumed.

The positive effects of an electric field on the ice formation have been reported (Shichiri and Nagata 1981; Shichiri and Araki 1986; Petersen et al., 2006; Sun et al., 2006, 2008; Orlowska et al., 2009). The nucleation temperature shifted towards higher values as an applied electrostatic field strength increases (Sun et al., 2008; Orlowska et al., 2009). With an alternative electric field, the ice crystallization properties, such as the degree of supercooling, freezing time and ice crystal size are controllable with working frequencies (Sun et al., 2006, 2008). The transient pulsed electric field (PEF) was also suggested as an alternative to deliver the same effect via alternative electric field of sinusoidal waveform (Sun et al., 2008). However, the basic mechanism of electric field on the ice crystallization is still contentious and most of the most of previous studies are limited to small volume of

water or slice of meats (Ade-Omowaye et al., 2003; Amami et al., 2006; Ammar et al., 2010; Jalté et al., 2009; Xanthakis et al., 2013).

Theoretical and experimental results showed that the magnetic field can make impacts on water structures (Aleksandrov et al., 2000; Woo and Mujumdar 2010; Iwasaka et al., 2011). The hydrogen bonds between water molecules are stronger and form a more ordered configuration under the magnetic field (Cai et al., 2009). This results in the formation of homogeneous ice crystals and enables the control of the sample cooling rate and the rate of crystal growth after nucleation (Norio and Satoru, 2001). Thus, the magnetic field can be one of the possible technologies involving cooling and freezing the sample. However, there are neither sufficient data nor detailed description for underlying mechanisms.

Recently, electromagnetic stresses by using microwave or radiofrequency have been introduced as an emerging food freezing technique. The underlying mechanism was that the electric field component of electromagnetic radiation would interact with dipolar water molecules, resulting in disruption of the ice nucleation and/or formation of small ice crystals (Jackson et al., 1997; Anese et al., 2012). All of the above mentioned emerging technologies involving ice formation can hold great potential techniques for improving the quality of frozen materials by controlling ice formation. However, there have existed critical challenges for the developed techniques to be expanded and scaled up for commercial applications.

1.2.7. Combination technologies

Although a large number of researchers have studied the effects of various freezing technologies on food qualities, less is known about the combination effect (or hurdle effect) of different emerging technologies on the quality of foods at frozen states. The application of a deliberate and intelligent combination of emerging technologies, which may also be simple hurdles with conventional preservation factors (e.g. temperature, water activity, redox potential, electrical conductivities), would be beneficial for effective freezing methods. With combined treatments, synergies are more achievable when individual treatments aim for different functionalities within the freezing processes. Moreover, a gentler preservation treatment enables with less damages on the quality of food products.

Among attainable combinations of emerging technologies, external electric field and magnetic field may have great potentials for the freezing process by non-thermal mechanisms. The effect of electric field on the ice formation due to the dipolar vibration and re-orientation has been addressed (Shichiri and Nagata, 1981; Shichiri and Araki 1986; Petersen et al., 2006; Sun et al., 2006, 2008; Orlowska et al., 2009; Woo and Mujumdar, 2010). Diamagnetic properties of water molecules under the magnetic field were intensively studied. (Aleksandrov et al., 2000; Iwasaka et al., 2011) Therefore, the combination of electric field and magnetic field can be utilized to minimize the damage on food tissues. Recently in Japan, new freezing system using electric and magnetic field combination was developed (Iwasaka et al., 2011). However, there is still no sufficient clarification for their underlying mechanisms to control the freezing process.

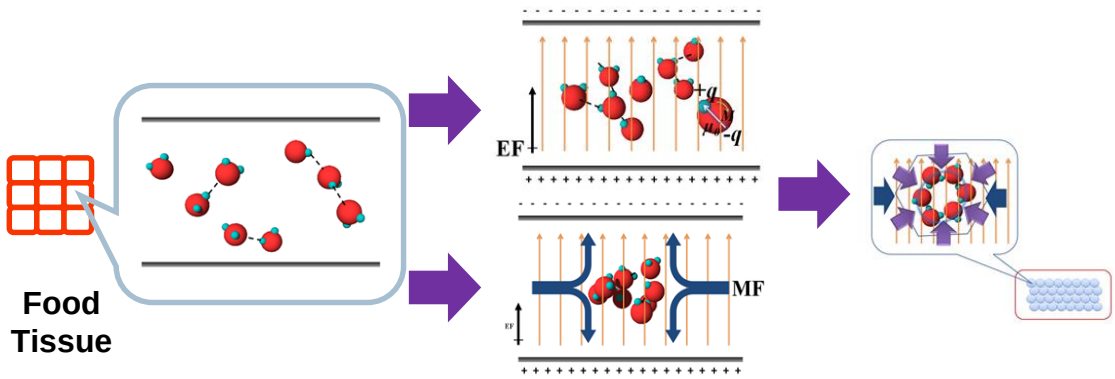

Figure 1.4. Schematic diagram of combination of electric field (EF) and magnetic field (MF). +*q* and -*q*: a pair of equivalent charges; μ_0: dipole moment; *M*: force moment exerted on the dipole.

Therefore, we hypothesized (1) that the pulsed electric field would cause water molecules to be polarized and re-orientated, and vibrations by magnetic flux would interrupt critical ice nucleation due to unique diamagnetism of water molecules and (2) that combination of pulsed electric and magnetic fields would result in finer ice formation or liquid phase on 'supercool' hold in food matrix, leading to full retention of food quality (Fig. 1.4).

1.3. Conclusion

This chapter offers mechanisms and properties of the phase transition from water to ice, which is a key part of food freezing processes. Freezing is not a process that improves the intrinsic qualities of food product but most efficient way to preserve food products over time. Thus, the challenge of the freezing process is to reduce the rate of physicochemical deterioration of final frozen food quality through improved storage conditions, which is close to raw material characteristics.

Through a thorough review of relevant literatures, there is a need for further studies on the development of emerging freezing technologies for practical applications. To aim this, the combination could be a great approach to offer the optimized conditions during supply, manufacture, and storage to preserve the quality and characteristics of fresh foods in the frozen product.

1.4. Overview of Thesis

Most of suggested emerging freezing technologies above have aimed to generate the small ice crystals via (i) instant nucleation based on pressure-temperature function or (ii) control the size and distribution of ice crystals by external stress.

The first part of the thesis is aimed to generate small ice crystals, which can minimize the structural damages on food tissues by freeze-cracking. The effects of water dipole reorientation induced by pulsed electric field (PEF) on ice crystals size and distribution during freezing were studied. The effects of magnetic field using permanent magnets on ice morphology were also explored. From the findings under two different treatments, the effects of the proposed freezing combination technique were examined. Although there are no or little relevant literatures, the similar effects of the application of electromagnetic stresses was expected.

The second part of the thesis begins with the understanding of anomalies of water, particularly, supercooling phenomenon. In order to overcome the randomness of the ice nucleation from supercooling state, the PEF and oscillating magnetic field (OMF) were applied to induce reorientation and vibration motion of water molecules. The combination of PEF and OMF was so effective to suppress the ice nucleation. Based on these findings,

the PEF and OMF combination was optimized to extend the supercooling state in foods. The results of tests using chicken breasts showed that supercooling state was significantly extended with an increase in the degree of supercooling. The quality factors were examined and compared with the control data to validate the effect of supercooling state on qualities of chicken breasts.

1.5. References

Ade-Omowaye, B.I.O., Rastogi, N.K., Angersbach, A., Knorr, D., 2003. Combined effect of pulsed electric field pre-treatment and partial osmotic dehydration on air drying behaviour of red bell pepper. J. Food Eng. 60, 89-98.

Aleksandrov, V.D., Barannikov, A.A., Dobritsa, N.V., 2000. Effect of magnetic field on the supercooling of water drops. Inorg. Mater. 36, 895-898.

Amami, E., Vorobiev, E., Kechaou, N., 2006. Modelling of mass transfer during osmotic dehydration of apple tissue pre-treated by pulsed electric field. LWT-Food Sci. Technol. 39, 1014-1021.

Ammar, J.B., Lanoisellé, J.L., Lebovka N.I., Van Hecke E., Vorobiev E., 2010. Effect of a pulsed electric field and osmotic treatment on freezing of potato tissue. Food Biophys. 5, 247-254.

Anese, M., Manzocco, L., Panozzo, A., Beraldo, P., Foschia, M., Nicoli, M.C., 2012. Effect of radiofrequency assisted freezing on meat microstructure and quality. Food Res. Int. 46, 50-54.

Angell, C.A., 1983. Supercooled water. Annu. Rev. Phys. Chem. 34, 593-630.

Barbosa-Cánovas G.V., Altunaker B., Mejía-Lorío D. J., 2005. FAO agricultural services bulletin/FAO. 158: Freezing of fruits and vegetables - An agribusiness alternative for rural and semi-rural areas. Rome, Italy. pp. 17-26.

Bartell, L.S., Huang, J., 1994. Supercooling of water below the anomalous range near 226 K. J. Phys. Chem. 98, 7455-7457.

Bigg, E.K., 1953. The supercooling of water. Proc. Phys. Soc. B 66, 688-694.

Cai, R., Yang, H., He, J., Zhu, W., 2009. The effects of magnetic fields on water molecular hydrogen bonds. J. Mol. Struct. 938, 15-19.

Campañone, L.A., Salvadori, V.O., Mascheroni, R.H., 2001. Weight loss during freezing and storage of unpackaged foods. J. Food Eng. 47, 69-79.

Canet, W., 1989. Quality and stability of frozen vegetables. in: Thorne, S. (Ed.), Developments in Food Preservation, vol. 5. Elsevier Science Publishing Inc., New York. pp. 1-50.

Chevalier, D., Sentissi, M., Havet, M., Le-Bail, A., 2000c. Comparison of air-blast and pressure shift freezing on Norway lobster quality. J. Food Sci. 65, 329-333.

Fennema O.R., 1977. Loss of vitamins in fresh and frozen foods. Food Technol.-Chicago 12, 32-38.

Giannakourou, M.C., Taoukis, P.S., 2003. Kinetic modelling of vitamin C loss in frozen green vegetables under variable storage conditions. Food Chem. 83, 33-41.

Gonçalves, E.M., Pinheiro, J., Abreum M., Brandãom, T.R.S., Silva, C.L.M., 2011. Kinetics of quality changes of pumpkin (*Curcurbita maxima L.*) stored under isothermal and non-isothermal frozen conditions. J. Food Eng. 106, 40-47.

Goyer, G.G., Bhadra, T.C., Gitlin, S., 1964. Shock induced freezing of supercooled water. J. Appl. Meteorol. 4, 156-160.

Hartel, R.W., 2001. Crystallization in foods. Aspen Publishers, USA.

Hu, S.Q., Liu, G., Li, L., Li, Z.X., Hou, Y., 2013. An improvement in the immersion freezing process for frozen dough via ultrasound irradiation. J. Food Eng. 114, 22-28.

Iwasaka, M., Onishi, M., Kurita, S., Owada, N., 2011. Effects of pulsed magnetic fields on the light scattering property of the freezing process of aqueous solutions. J. Appl. Phys. 109, 07E320.

Jackson, T.H., Ungan, A., Critser, J.K., Gao, D., 1997. Novel microwave technology for cryopreservation of biomaterials by suppression of apparent ice formation. Cryobiology 34, 363-372.

Jalté, M., Lanoisellé, J.L., Lebovka, N.I., Vorobiev, E., 2009. Freezing of potato tissue pre-treated by pulsed electric fields. LWT-Food Sci. Technol. 42, 576-580.

Kashiwagi, T., Hirose, S., Itoh, S., Kurosaki, Y., 1987. Effects of the natural convection in a partially supercooled water cell on the release of supercooling. Trans. JSME 53, 1822-1827.

Le-Bail, A., Chevalier. D., Mussa, D.M., Ghoul, M., 2002. High pressure freezing and thawing of foods: a review. Int. J. Refrig. 25, 504-513.

Li, B., Sun, D., 2002. Novel methods for rapid freezing and thawing of foods - a review. J. Food Eng. 51, 175-182.

Luque de Castro, M.D., Priego-Capote, F., 2007. Ultrasound assisted crystallization (sonocrystallization). Ultrasonic Sonochem. 14, 717-724.

Martins, R.C., Silva, C.L.M., 2002. Modelling colour and chlorophyll losses of frozen green beans (*Phaseolus vulgaris*, L.). Int. J. Refrig. 25, 966-974.

Mason, T.J., Paniwnyk, L., Lorimer, J.P., 1996. The use of ultrasound in food technology. Ultrasonic Sonochem. 3, 253-260.

Mazur, P., 1984. Freezing of living cells-mechanisms and implications. Am. J. Physiol. 247, C125-142.

Norio, O., Satoru, K., Inventors; ABI Limited, assignee. 2001 Jun 26. Super-quick freezing method and apparatus therefore. U.S. patent 6,250,087 B1.

Norton, T., Sun, D.W., 2008. Recent advances in the use of high pressure as an effective processing technique in the food industry. Food Bioprocess Tech. 1, 2-34.

Orlowska, M., Havet, M., Le-Bail, A., 2009. Controlled ice nucleation under high voltage DC electrostatic field conditions. Food Res. Int. 42, 879-884.

Otero, L., Sanz, P.D., 2000. High-pressure shift freezing. Part 1. Amount of ice instantaneously formed in the process. Biotechnol. Progr. 16, 1030-1036.

Persson, P.O., Londahl, G., 1993. Freezing technology, in: Mallett, C.P. (Ed.), Frozen food technology. Blackie Academic & Professional Inc., Glasgow, UK, pp. 20-58.

Petersen, A., Schneider, H., Rau, G., Glasmacher, B., 2006. A new approach for freezing of aqueous solutions under active control of the nucleation temperature. Cryobiology 53, 248-257.

Petrenko, V.F., Withworth, R.W., 1999. In: Physics of ice, Oxford University Press, New York.

Pilar Cano. M., 1999. Vegetables. In: Jeremiah, L.E. (Ed.), Freezing effects on food quality. New York: Marcel Dekker Inc., pp. 247-297.

Powrie, W.D., 1984. Chemical effects during storage of frozen foods. J. Chem. Educ. 61, 340-347.

Saito A., Okawa, S, Tojiki, A., Une, H., Tanogashira, K., 1992. Fundamental research on external factors affecting the freeing of supercooled water. Int. J. Heat Mass Tran. 35, 2527-2536.

Schlüter, O., Urrutia Benet, G., Heinz, V., Knorr, D., 2004. Metastable states of water and ice during pressure-supported freezing of potato tissue. Biotechnol. Progr. 20, 799-810.

Schlüter, O., Foerster, J., Geyer, M., Knorr, M., Herppich, W.B., 2009. Characterization of high-hydrostatic-pressure effects on fresh produce using chlorophyll fluorescence image analysis. Food and Bioprocess Tech. 2, 291-299.

Schulson, E.M., 1999. The structure and mechanical behavior of ice. J. Min. Met. Mat. 51, 21-27.

Shaw, R.A., Durant, A.J., Mi, Y., 2005. Heterogeneous surface crystallization observed in undercooled water. J. Phys. Chem. B 109, 9865 – 9868.

Shichiri, T., Nagata, T., 1981. Effect of electric currents on the nucleation of ice crystals in the melt. J. Cryst. Growth 54, 207-210.

Shichiri, T., Araki, Y., 1986. Nucleation mechanism of ice crystals under electrical effect. J. Cryst. Growth 78, 502-508.

Soyer, A., Özalp, B., Dalmış, Ü., Bilgin, V., 2010. Effects of freezing temperature and duration of frozen storage on lipid and protein oxidation in chicken meat. Food Chem. 1210, 1024-1030.

Stokely, K., Mazza, M.G., Stanley, H.E., Franzese, G., 2010. Effect of hydrogen bond cooperativity on the behavior of water. PNAS 107, 1301-1306.

Sun, W., Xu, X., Sun, W., Ying, L., Xu, C. Effect of alternated electric field on the ice formation during freezing process of 0.9% K_2MnO_4 water. IEEE 8th International Conference on; 2006 June 26-30; Bali, Indonesia: Properties and applications of Dielectric Materials; c2006.

Sun, W., Xu, X., Zhang, H., Sun, W., Xu, C. The Mechanism Analysis of NaCl Solution Ice Formation Suppressed by Electric Field. IEEE 8th International Conference on; 2006 June 26-30; Bali, Indonesia: Properties and applications of Dielectric Materials; c2006.

Sun, W., Xu, X., Zhang, H., Xu, C., 2008. Effects of dipole polarization of water molecules on ice formation under an electrostatic field. Cryobiology 56, 93-99.

Tanaka, H., 2000. Simple physical model of liquid water. J. Chem. Phys. 112, 799-809.

Tolbert, S.H., Alivisatos, A.P., 1995. High pressure phase transitions in semiconductor nanocrystals. Annu. Rev. Phys. Chem. 46, 595-625.

Turnbull, D., 1956. Phase Change, in: Seitz, F., Turnbull, D., (Eds.), Solid State Physics, vol. 2. Academic Press Inc., New York, pp. 226-306.

Virone, C., Kramer, H.J.M., van Rosmalen, G.M., Stoop, A.H., Bakker, T.W., 2006. Primary nucleation induced by ultrasonic cavitation, J. Crystal Growth 1, 9-15.

Woo, M.W., Mujumdar, A.S., 2010. Effects of electric and magnetic field on freezing and possible relevance in freeze drying. Dry Technol. 28, 433-443.

Xanthakis, E., Havet, M., Chevallier, S., Abadie, J., Le-Bail A., 2013. Effect of static electric field on ice crystal size reduction during freezing of pork meat. IFSET, In press.

Zachariassen, K.E., Kristiansen, E., Pedersen, S.A., 2004. Inorganic ions in cold-hardiness. Cryobiology 48, 126-133.

Zhang, S., Wang, H., Chen, G., 2010. Addition of ice-nucleation active bacteria: *pseudomonas syringae* pv. *panici* on freezing of solid model food. LWT - Food Sci. Technol. 43, 1414-1418.

CHAPTER 2

EMERGING PULSED ELECTRIC FIELD (PEF) AND STATIC MAGNETIC FIELD (SMF) COMBINATION TECHNOLOGY FOR FOOD FREEZING

2.1. Abstract

The potential of an innovative freezing technique by applying combined pulsed electric field (PEF) and static magnetic field (SMF) was successfully tested and validated. 0.9% sodium chloride (NaCl) solution was frozen under the PEF (1.78 V/cm, duty cycle: 0.5) at the frequencies of 0-20 kHz and different SMF conditions (attractive and repulsive). At freezer temperature of -20°C, an increase in the working frequencies reduced the phase transition time and the shortest phase transition time (1443 ± 2 sec) was obtained at 20 kHz. The patterns of ice crystals became uniformly round (roundness: 0.88-0.90) under the PEF. The effects of attractive and repulsive SMFs showed different patterns in ice crystal formation with the shortest phase transition time under the repulsive SMF. The combined PEF (1.78 V/cm at 20 kHz) and repulsive SMF resulted in an effective and synergistic freezing process with the shortest phase transition (1004 ± 3 sec), forming the round and finest ice crystals (equivalent diameter: 97 ± 12 μm; roundness: 0.90 ± 03; elongation: 1.24 ± 0.33).

2.2. Introduction

Freezing plays an essential role in ensuring the safety of food products and retaining the quality of foods over long storage periods. Nonetheless, the consequences of freezing and thawing remain a significant problem on the quality of foods. During the freezing

process, ice crystallization can result in irreversible damages to tissue structures such as structural ruptures and changes in osmotic pressure due to the overshoot of extracellular concentration of solutes as ice freezes out (Mazur, 1984). It also changes the sensory properties of foods after deliveries and storages. Thus, it is important to control the size and location of ice crystals within food products under proper storage conditions.

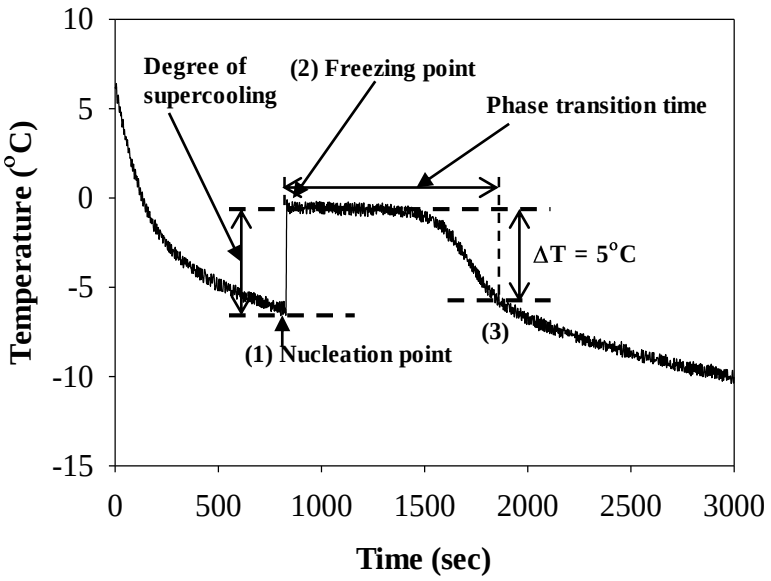

Figure 2.1. A typical temperature profile of water freezing: (1) nucleation point and (2) freezing point. The difference between the (1) and (2) is the degree of supercooling. The time lag between (1) and (3) is defined as the phase transition time.

The ice crystallization process can be divided into three subsequent stages; cooling the liquid-state product to its freezing point, removing the latent heat of crystallization during the phase transition, and cooling the solid-state product to the final storage temperature. Figure 2.1 shows a typical temperature profile of ice crystallization. As the

water sample cools down, it enters the supercooled region. Water temperature drops down until a critical nucleation point is reached by the removal of sensible heat. The negative difference between the nucleation point ((1) in Fig. 2.1.) and freezing point (2) is called as a degree of supercooling. After a certain degree of supercooling, a sudden nucleation of water crystals occurs by loss of sensible heat from the water molecules. Thereafter, the ice crystals become more compact and undergo the critical phase change (crystallization). The phase transition time is defined as the time it takes for the ice crystals to undergo the phase change and the temperature to drop down to 5°C from the freezing point (3). Lots of research efforts have been made to shorten the freezing period, increase the freezing rate, and maintain temperature stability during freeze-storage. Alternative techniques include ultrasound-assisted food freezing (Chow et al., 2005; Saclier et al., 2010), high-pressure shift food freezing (Norton and Sun, 2008; Otero et al., 2009), ice nucleating proteins (Zhang et al., 2010), antifreeze proteins (Li and Sun, 2002), superchilling technology (Magnussen et al., 2008), and Cell Alive System (CAS) technology, which has known to electromagnetic fields-based system ("Cell Alive System (CAS) technology for the idealistic foods", 2011).

Although a large number of researchers have studied various freezing technologies for improvement of frozen food quality, the developed technologies have neither incorporated corollary in theory nor fully explored for practical application. Therefore, the combination of different emerging technologies was introduced to resolve these problems. The synergies from strategically combined treatments are more achievable when individual treatments share different functions within freezing processes, with minimized damages on the quality of food products.

Among attainable combinations of emerging technologies, external electric field and magnetic field were tested and expected to enhance the initiation of small ice crystals to minimize the damage on food tissues. Recently in Japan, new freezers, utilizing the eclectic and magnetic fields, became commercialized (Iwasaka et al., 2011). However, there is no sufficient clarification for their underlying mechanisms to control the freezing process.

In this study, the transient pulsed electric field (PEF) was used to figure out its effect on freezing process similar to previous studies (Shichiri and Nagata, 1981; Shichiri and Araki 1986; Petersen et al., 2006; Sun et al., 2006, 2008; Orlowska et al., 2009; Woo and Mujumdar, 2010). The PEF is well known to manipulate the physical and chemical characteristics of treated products depending upon its pulse wave shape, frequency and processing temperature (Samaranayake et al., 2005; Shim et al., 2010). However, most researches till date focus on the use of new technologies on the pre-treatments prior to freezing. Further research is required to see the effect of the use of these technologies during actual freezing process (Ade-Omowaye et al., 2003; Amami et al., 2006; Jalté et al., 2009; Ammar et al., 2010).

In later part of this report, the PEF and SMF combination treatment was tested for optimization of ice crystallization and the results were analyzed by the microstructures of ice crystals and the temperature profiles.

2.3. Materials and Methods

2.3.1. Freezing cell system

Figure 2.2 shows a set of experimental apparatus consisting of a pulse function generator, a pair of parallel electrode bars, a cooling chamber and a real-time temperature measurement system. The power supply based on an integrated-gate-bipolar-transistor (IGBT, SKYPER^{TM}, SEMIKRON Inc., Hudson, NH) was designed to generate pulsed square waveform in a range between 0-20 kHz. Two titanium electrodes (2 mm in thickness (t), 40 mm in length (l) and 5 mm in height (h)) were located at a horizontal and parallel position onto glass slide with 14 mm gap to observe the ice crystals via a microscope. The fabricated cell was designed to test 2 ml of solution samples. K-type thermocouple wire (K-type, PP-K-24S, Omega Engineering, Inc., Stamford, CT) aligned at the center of the cell was used to measure sample temperature. Two of Ultem 1000 polyetherimide blocks (AIN Plastics of Ohio, Inc., Columbus, OH) were engraved to load the disc magnet (diameter d = 38.1 mm and t = 12.7 mm) at the center and adjusted by tightening the bolts with nuts when dealing with the positioning and alignment of the cell. Two of grade N52 neodymium (NdFeB) permanent disc magnets (DX88-N52, K & J Magnetics, Inc., Jamison, PA) were fixed on the blocks and covered by acrylic plate supports. The magnetic flux densities between each magnet at top-and-bottom configurations was measured using a handheld teslameter (4060.50 AE Teslameter, Frederiksen, Inc., Ølgod, Denmark). The fabricated cell device with electric and magnetic fields was placed in the chest freezer. A data acquisition unit (DAQ, Agilent 39704A, Agilent Technologies, Inc., Palo Alto, CA) was used to measure and monitor the applied voltage and current, and temperature values

of solutions and air in a freezer. The data were scanned and transmitted at the interval of 1 sec. All samples were specifically placed at the same position for each experiment.

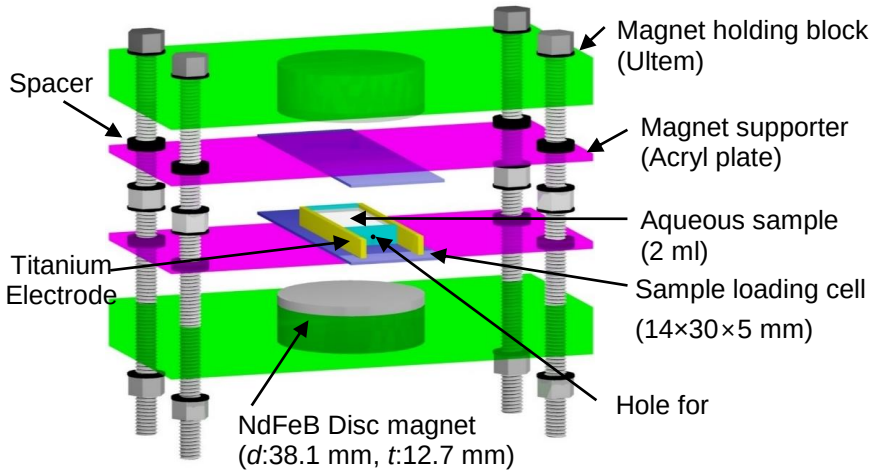

Figure 2.2. A schematic diagram of the fabricated freezing device. 2 ml of sample was placed in the cell. Two disc magnets were placed in magnet holding blocks and fixed by acryl plates. The voltage was applied between the titanium electrodes for PEF.

2.3.2. PEF and SMF treatments

The applied PEF strength was set at 1.78 V/cm with a fixed on/off duty cycle of 0.5, where there would be no electro-conductive heating involved. Various working frequencies at the ranges between 1 and 20 kHz were set and tested to validate the frequency impacts on the ice crystallization: ice crystal patterns and phase transition times. Experiments without applied PEF were performed as a reference to the measurements conducted under the PEF. The freezer temperatures were set at -7, -8.5, -10, -11.5 and -20°C to investigate the influence of the PEF on the degree of supercooling and, consequently, on the ice crystal sizes.

In order to study the influence of magnetic field on the ice crystallization of solution, ice crystal patterns and phase transition times were measured similar to the PEF treatment. The magnetic flux densities were ranged from 0 to 480 mT and adjusted by varying the pole distance between two magnets. Types of SMF were determined by changing the position of magnet poles (Either attractive or repulsive). In configuration-wise, since the motion of charged particles and diamagnetic molecules are ultimately influenced by the force directions (attraction or repulsion), the distances between two magnets were fixed as same under attractive and repulsive forces. Thus, magnetic flux densities indicate the interaction of two magnetic forces at the center of fabricated cell and they were estimated to 480 and 50 mT, respectively.

2.3.3. Sample preparation and freezing protocol

A 0.9% NaCl solution, considered as physiological and biological solution, has been used for this study. In all of the proposed experiments, each repetition prepared with new sample solution started with the pre-cooling step to make initial temperature of solution samples uniform and constant (5°C). Freezer temperature was stabilized in 30 min and then the sample solution was placed in the fabricated cell until it completed the phase transition and solidification processes.

2.3.4. Microscopic analysis

The size and morphology of ice crystals were important for validation of the combination freezing technique. The images from an optical microscope were captured using normal light-sensitive charge-coupled device (CCD) camera. The images were stored

and analyzed using Mshot Digital Microscope Imaging System v1.0. For each measurement, images at five different spots of frozen solutions were obtained and used for the subsequent image analysis.

The samples in the present paper were frozen with the samples used for evaluation of the ice crystal structures in the accompanying paper (Zhu et al., 2005). The ice crystal size was defined as the equivalent diameter of a circle having the same area as the targeted object. The roundness (R) was estimated as:

$$R = \frac{4\pi A}{p^2} \tag{2.1}$$

where A is the cross-section area (μm^2) and p is the perimeter (μm). The roundness has a value in the range 0-1, with a value of 1 for a circle. The elongation (e) was estimated by the ratio of major axis length to the minor axis length. A shape symmetrical in all axes such as a circle or square has an elongation value of 1 whereas elongated shapes with large aspect ratios have an elongation value higher than 1. Using the data obtained from more than 30 ice crystals in each case, analysis of variance (ANOVA) routine used to test the significance of the dissimilarities between the means of testing parameters among the treatments ($P < 0.05$).

2.4. Results and Discussion

2.4.1. PEF treatment: Frequency

The PEF strength of 1.78 V/cm with 0.5 duty cycle at various working frequencies were applied to NaCl solution at -20ºC to test the effects of frequencies of PEF on ice crystallization. Figure 2.3 shows the changes in the phase transition time, in which the

solution becomes frozen completely, in different frequencies and the representative micrograph of solution samples frozen at 20 kHz, which was the max frequency used in this study. The phase transition time decreased with an increase in the working frequencies showing high correlation (R^2 = 0.968, Fig. 2.3(a)). The shortest phase transition time was 1443 ± 2 sec at 20 kHz. The dependence of phase transition time on the frequency was also observed for sinusoidal electric field treatments (Sun et al., 2006). Based on the polarities of alternative electric field, polarization and reorientation of water dipole molecules result in vibration and collision of those molecules. Induced vibration and collision generate the thinner solid–liquid boundaries and decrease heat transfer resistance (Hu et al., 2013).

The rapid heat transfer results in the smaller ice crystal size with dense clusters and the shorter phase transition time under the PEF than control (Fig. 2.3(b)). Compared to the sinusoidal electric field (28.6%, calculated from Sun et al., 2006), the pulsed electric field reduced the phase transition time by 34.8%. This observation could be because the rectangular pulses produce quick realignment of water molecules and offer stronger bonds in parallel to the electric field, similar to the DC electrostatic field (Orlowska et al., 2009). The bond breaking and reformation of water molecules by external electric field accelerates the molecular vibration and create the ordered ice forms, leading to shortened phase transition time and uniform ice crystals (Vegiri, 2004). Thus, the amount of reduction in phase transition times can be different depending upon the waveforms of the alternative electric fields and PEF would be the most effective on reduction of phase transition time.

(a)

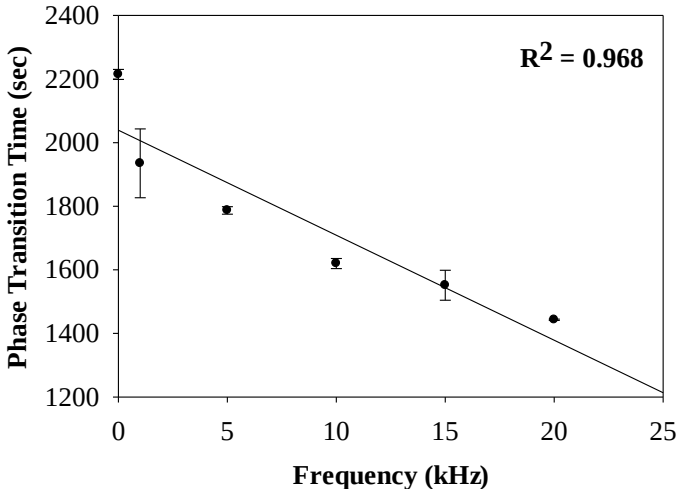

(b)

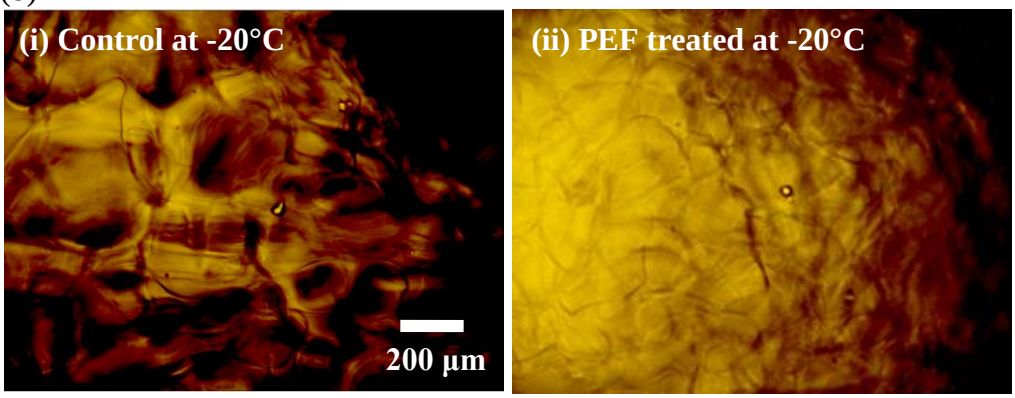

Figure 2.3. The effect of PEF on ice crystallization by changing working frequencies. (a) The phase transition times correlated with the frequencies of PEF and (b) representative corresponding micrographs of solution frozen (i) without and (ii) with working frequency (20 kHz) at -20ºC. R^2 = 0.968. Mean values ± standard deviation (S.D.) of three replicated measurements.

2.4.2. PEF treatment: Degree of supercooling (ΔT_{sc}) and surrounding temperature

The effects of PEF on the degree of supercooling (ΔT_{sc}) of sample solutions were investigated. In order to clarify the effect of PEF application, the experiment were carried

out using NaCl solutions without PEF and the ΔT_{sc} was estimated to 1.7 ± 0.3°C at any freezer temperature settings between -7 and -11.5°C. Since the supercooling phenomenon is a function of temperature (Zaritzky, 2011), the values of ΔT_{sc} could be controlled by the surrounding temperature. The temperatures of freezing chamber tested in this study were -7, -8.5, -10, and -11.5°C. From the findings previous section, the PEF strength of 1.78 V/cm with 0.5 duty cycle at 20 kHz were applied to the same sample solution. Table 1 summarizes the statistical analysis of the ice crystals formed in different settings. Figure 2.4 shows the patterns of ice crystals observed under the microscope and the correlation of the ice crystal sizes with the degrees of supercooling. Compared to the control, the patterns of ice crystal under PEF were uniform and round, showing the roundness of 0.88-0.90 and less elongation, which is closer to circle. Also, ice crystals under the PEF showed narrow diameter distribution and it was confirmed by smaller standard deviation (S.D.) over the mean value (3.4%) than that of control (21.4%) (Fig. 2.4(a) and Table 2.1).

Table 2.1. Microscopic analysis results (mean ± S.D.) of the ice crystals frozen by various treatment conditions

Parameter	Equivalent diameter (μm)	Roundness (*R*)	Elongation (*e*)
Control (-11.5°C)	277 ± 134^{ab}	0.70 ± 0.15^{a}	2.00 ± 1.01^{a}
Control (-20°C)	178 ± 84^{cd}	0.68 ± 0.11^{a}	1.94 ± 0.51^{ab}
PEF (20 kHz, -7.0°C)	265 ± 30^{e}	0.90 ± 0.03^{b}	1.68 ± 0.42^{bc}
PEF (20 kHz, -8.5°C)	204 ± 20^{bf}	0.89 ± 0.03^{b}	1.55 ± 0.40^{def}
PEF (20 kHz, -10.0°C)	186 ± 16^{df}	0.90 ± 0.03^{b}	1.62 ± 0.44^{cf}
PEF (20 kHz, -11.5°C)	130 ± 13^{g}	0.88 ± 0.04^{b}	1.81 ± 0.32^{ef}
PEF (20 kHz, -20.0°C)	102 ± 24^{h}	0.90 ± 0.03^{b}	1.44 ± 0.49^{d}

In each column, dissimilar small letters in each column indicate significant difference at 0.05 levels.

(a)

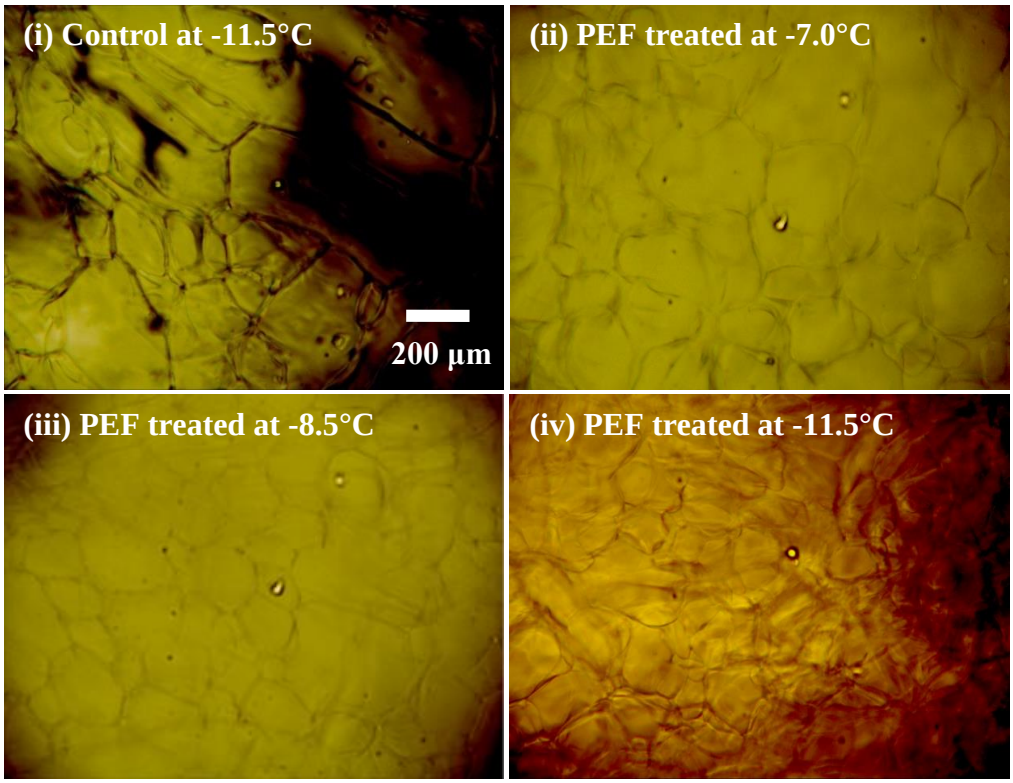

(b)

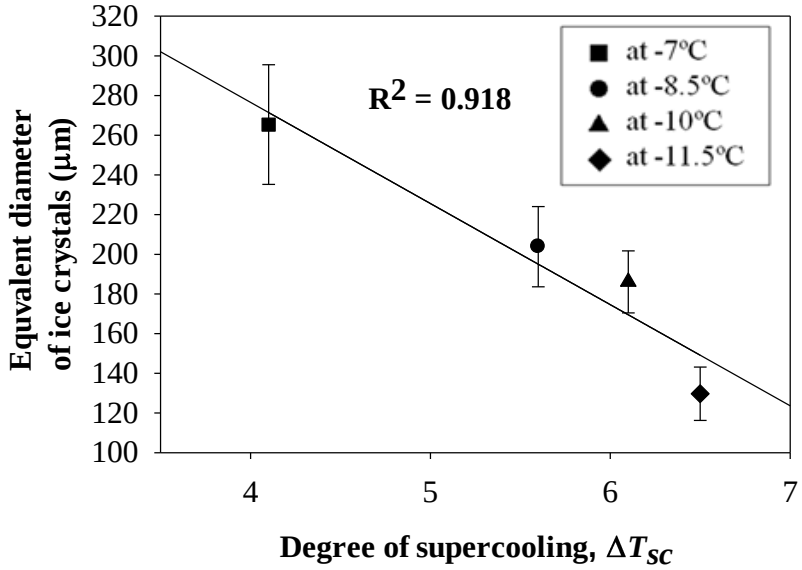

Figure 2.4. Effects of ΔT_{sc} on ice crystal sizes in the presence of PEF. (a) ice crystal sizes with and without PEF at freezer temperatures between -7 and -11.5°C and (b) ΔT_{sc} vs. ice crystal size in the presence of PEF. R^2=0.918.

The impact of PEF on the degree of supercooling is shown in Figure 2.4(b). Compared to control, the solution under the PEF showed increased ΔT_{sc} as decreased the freezer temperature settings and there was the largest ΔT_{sc} (6.5°C) obtained at -11.5°C. Thus, it can be inferred that there is a significant impact in the degree of supercooling when freezing was carried out in the presence of PEF. Since all of samples in this temperature range showed the same cooling rates and the phase transition time (data not shown), the lower nucleation point implies the longer period of solid–liquid equilibrium state. Thus, the longer supercooling resulted in smaller ice crystals and it was consistent with our findings with previous studies (Le-Bail, 2004).

These results also can be explained in kinetic approaches as well. The free energy (ΔG_E) needed for formation of a spherical nucleus can be applied to address the nucleation and growth of ice crystals in the presence of an electric field, as follows (Orlowska et al., 2009; Marand et al., 1998):

$$\Delta G_E = 4\pi r^2 \gamma - \frac{4}{3}\pi r^3 (\Delta G_v + PE) \tag{2.2}$$

where r is the radius of the nuclei sphere (m), γ is the surface free energy of the crystal fluid interface (J/m^2), E is the electric field strength (V/m), P is the polarization (C/m^2) and ΔG_v is the free energy of freezing per unit volume (J/m^3):

$$\Delta G_v = \frac{\Delta H_{m,f}(T_f - T)}{T_f V_m} \tag{2.3}$$

where $\Delta H_{m,f}$ is the molar enthalpy of fusion (J/mol), V_m is the molar volume (m^3/mol) and ($T_f - T$) represents the value of ΔT_{sc}. In supercooling state of water, when a set of water molecules join by chance, either of two cases, continuous formation or disintegration of small embryos of ice, could happen. If the ice embryo is below a critical size, the additional

linking of a new molecule is not energetically favorable, so the embryo disappears and supercooled water remains as liquid state. However, if the ice embryo is larger than this critical size, it might continue increasing in size up to a microscopic ice crystal. The critical size can be expressed as r^* given by:

$$r^* = \frac{2\gamma}{\Delta G_v + PE} \tag{2.4}$$

From the equation (2.4), under the assumption that the surface free energy of the crystal fluid interface is constant, it follows that the P and ΔT_{sc} can affect the critical nucleus radius, causing to larger population of smaller ice crystals. According to Ricinschi and Okuyama (2010), the polarization increased dramatically with increases in the frequencies of PEF with the same field intensities. Consequently, the critical radius was expected to dramatically decrease down by high PEF frequency, which was also consistent with our findings at the control and in the presence of PEF (Fig. 2.3(b) and Table 2.1). The theoretical effect of ΔT_{sc} on the critical radius proved by the simulation work of Olmo et al., (2008) was equally observed in our results with a linear correlation in limited temperature ranges (Figure 4(b)).

From the results at lower temperature than -11.5°C, there were no dependence of ΔT_{sc} on the surrounding temperature under both treatments, with and without PEF. Each pattern of ice crystals was similar to each treatment but the smallest ice crystals were generated at -20°C (Table 2.1). It might be a challenge to correlate the cooling rates with the sizes of ice crystals due to the complexity of the freezing process (Kiani and Sun, 2011). From our findings, the results proved that the cooling rate is one of key factors in consideration to determine the size of ice crystal.

2.4.3. SMF Treatment

Figure 2.5 shows attractive and repulsive forces applied to the sample solution at -20°C to compare ice morphology and phase transition time under magnetic fields. Compared to the control (Fig. 2.3(b)-(i)), ice crystals treated by the static magnetic field formed irregular shapes but different patterns based on the types of external forces. Due to diamagnetic properties of water and ionic interactions, Na^+ and Cl^- ions could cause the hydrogen bonding to be ruptured under the magnetic fields (Chang and Weng, 2008). Particularly, 'parting' pattern under the attractive SMF was derived from its unidirectional magnetic force (Fig. 2.5(a)) and diamagnetic properties of water. This force generates persistent atomic or molecular currents of water that would oppose externally applied magnetic fields (Ueno and Iwasaka, 1994; Simon et al., 2001). In the case of repulsive SMF, the outward field direction results in re-arrangement of the water molecules with sequential rotating effect and re-organization of Na^+ and Cl^- ions. In addition, molecular vibrations occur due to positioning of ions and molecules, which interferes with the rotation of molecules. Upon these changes by the repulsive SMF, both of the *van der Waals* bonding between water molecules and the interaction between ions and water molecules become weak. Thereafter, relatively free water molecules enhance the hydrogen bonding and their competition yields unique pattern of ice crystals (Chang and Weng 2006; Toledo et al., 2008 Bin et al., 2011), as resulting from our studies (Fig. 2.5(b)).

The effect of SMF was observed not only in the ice crystal shape but also the phase transition time. Compared to the control (2215 ± 16 sec) and attractive SMF (2593 ± 15 sec), the phase transition time in repulsive SMF (1504 ± 10 sec) was reduced by 32.1% and 42.0%, respectively. It should be noted that the phase transition time was elongated

when the attractive SMF was applied. This might be due to the likely distortion of hydrogen bonds, because unidirectional attractive magnetic field tends to form weaker polygonal rings such as hexagonal rings and rhombic rings. They also result in a shift of the second shell to the nearest neighbors in bilayer of ice, resulting in a longer freezing time (Zhang et al., 2010). It was clearly observed that different force directions and induced magnetic flux densities could enhance or change the anisotropies of water molecules and natures of ice crystals during the phase transition.

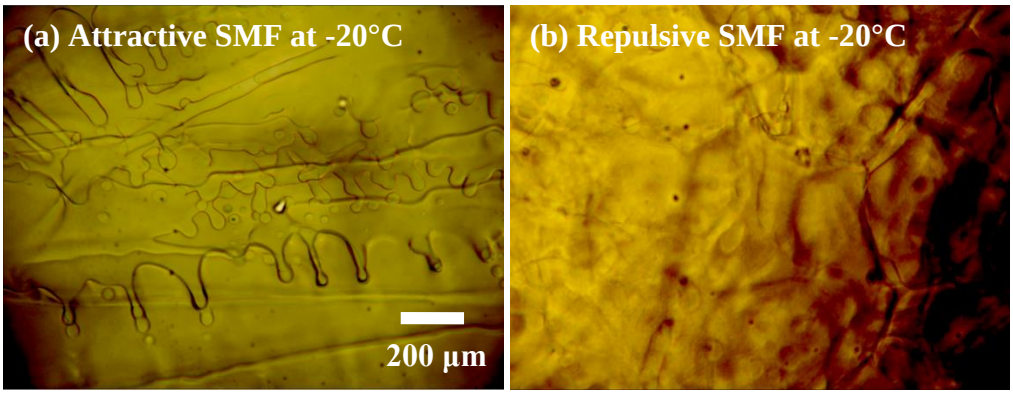

Figure 2.5. Microscopic images of ice crystals at -20°C under (i) attractive SMF (480 mT) and (ii) repulsive SMF (50 mT).

2.4.4. Ice crystallization under the combined PEF and repulsive SMF treatment

Based on the results of individual treatment of PEF and SMF, both of treatments showed enhanced by unique patterns of ice crystals and changes in phase transition time. Since both of treatments have different mechanisms to control the ice crystallization, the influence of combination of PEF and SMF were tested.

(a)

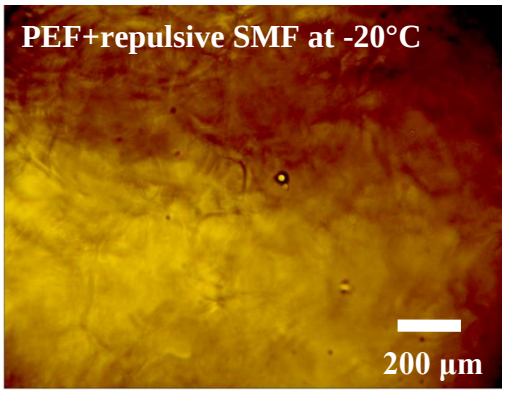

(b)

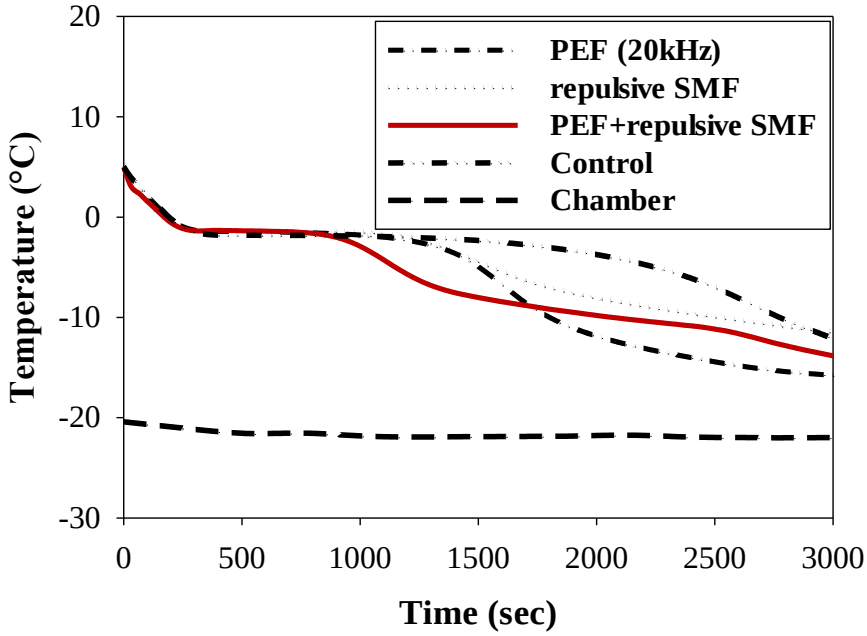

Figure 2.6. The effect of combination of PEF at 20 kHz and repulsive SMF on ice crystallization. (a) Microscopic images of ice crystals at -20°C under combination of PEF and repulsive SMF (PEF+repulsive SMF) and (b) The freezing curves under various treatments at ambient temperature (-20°C).

The effect of combined freezing treatments was also validated using microscopic image and freezing curve (Fig. 2.6). The same roughness under the repulsive SMF and uniform and round patterns of ice crystals by the PEF were observed. The estimated

equivalent diameter, roundness and elongation was 97 ± 12 μm, 0.90 ± 0.04, and 1.24 ± 0.33, respectively. The water molecules were disturbed and delocalized by the repulsive SMF and formed uniform patterns of ice crystals by the applied PEF. The movements of the charged particles in the aqueous NaCl solutions were enhanced by the perpendicular combination of external SMF and PEF, similar to the simulation result of the Lorentz force clarifying that water molecules become more stable and ions get unsteady by changing their directions without gaining or loss of energy (Chang and Weng, 2008).

With the same cooling rate, the phase transition times estimated for the control, PEF, repulsive SMF, and combined PEF and repulsive SMF treatments were 2215 ± 16, 1443 ± 2, 1504 ± 10, 1004 ± 3 sec, respectively (Fig. 2.6(b)). The reduction percentiles of the phase transition times for the control, individual PEF and repulsive SMF treatment in comparison to the combination freezing technique were 54.7%, 33.2%, and 30.4%, respectively.

In this context, the demonstrated combination of PEF and repulsive SMF displayed the synergistic effects. Thereby, the experimental results showed a potential for the practical use in the food processing to improve the quality of frozen foods by enhancement of uniform and desirable ice morphology. A mathematical approach is needed for better understanding of the effects of electric field and magnetic field on the freezing process and optimization of the process parameters, including kinetic variables for energy and mass transport phenomena. The next step in this study will be to develop a comprehensive model for supercooling and phase transition time, and to validate model predictions with the experimental measurements.

2.5. Conclusion

The present study revealed the significant impact of the external PEF and SMF on freezing of 0.9% NaCl solution. In the presence of the PEF, the solutions had a tendency to form uniform, fine and round ice crystals. Under the freezing condition at -20°C, the high frequency of PEF reduced the phase transition time. The repulsive SMF also led to shorter phase transition time and uniform ice crystal patterns. Under the combination of PEF and repulsive SMF, the phase transition time decreased remarkably. Even roughness, and uniform and round patterns of ice crystals were observed under the repulsive SMF and the PEF, respectively. Findings of the current study demonstrate the suitable processing strategy to maintain the freshness of food products with increased storage lives. Therefore, future studies could include model development for prediction of the freezing time of real foods (i.e. meats, potatoes, strawberries) and optimization of the freezing conditions with minimum quality loss of food products.

2.6. References

Ade-Omowaye, B.I.O., Rastogi, N.K., Angersbach, A., Knorr, D., 2003. Combined effect of pulsed electric field pre-treatment and partial osmotic dehydration on air drying behaviour of red bell pepper. J. Food Eng. 60, 89-98.

Aleksandrov, V.D., Barannikov, A.A., Dobritsa, N.V., 2000. Effect of magnetic field on the supercooling of water drops. Inorg. Mater. 36, 895-898.

Amami, E., Vorobiev, E., Kechaou, N., 2006. Modelling of mass transfer during osmotic dehydration of apple tissue pre-treated by pulsed electric field. LWT-Food Sci. Technol. 39, 1014-1021.

Ammar, J.B., Lanoisellé, J.L., Lebovka N.I., Van Hecke E., Vorobiev E., 2010. Effect of a pulsed electric field and osmotic treatment on freezing of potato tissue. Food Biophys. 5, 247-254.

Bin, G., Hai-bo, H., Feng, C., 2011. Influence of magnetic field on microstructural and dynamic properties of sodium, magnesium and calcium ions. Trans. Nonferrous Met. Soc. China 21, s494-498.

Carapelle, A., Henrist, M., Rabecki, F., 2001. A study of freeze-drying of frozen wet papers. Drying Technol. 19, 1113-1124.

Cell Alive System (CAS) technology for the idealistic foods [Internet]. Tokyo, Japan: PROJECT BANK; 2011-2012 [Updated 2011 Jun 20; Accessed 2012 Oct 24]. Available from: http://www.a-interview.com/en/world/item/92.html.

Chang, K.T., Weng, C.I., 2006. The effect of an external magnetic field on the structure of liquid water using molecular dynamics simulation. J. Appl. Phys. 100, 043917.

Chang, K.T., Weng, C.I., 2008. An investigation into the structure of aqueous NaCl electrolyte solutions under magnetic fields. Comp. Mater. Sci. 43, 1048-1055.

Chow, R., Blindt, R., Chivers, R., Povey, M., 2005. A study on the primary and secondary nucleation of ice by power ultrasound. Ultrasonics 43, 227-230.

Hu, S.Q., Liu, G., Li, L., Li, Z.X., Hou, Y., 2013. An improvement in the immersion freezing process for frozen dough via ultrasound irradiation. J. Food Eng. 114, 22-28.

Iwasaka, M., Onishi, M., Kurita, S., Owada, N., 2011. Effects of pulsed magnetic fields on the light scattering property of the freezing process of aqueous solutions. J. Appl. Phys. 109, 07E320.

Jalté, M., Lanoisellé, J.L., Lebovka, N.I., Vorobiev, E., 2009. Freezing of potato tissue pre-treated by pulsed electric fields. LWT-Food Sci. Technol. 42, 576-580.

Kiani, H., Sun, D.W., 2011. Water crystallization and its importance to freezing of foods: A review. Trends Food Sci. Tech. 22, 407-429.

Le-Bail A., 2004. Freezing processes, in: Hui, Y. H., Cornillon P., Legaretta, I. S., Lim, M. H., Murrell, K. D., Nip, W. K., (Eds.), Handbook of frozen foods. Marcel Dekker Inc., New York, pp. 1-11.

Li, B., Sun, D.W., 2002b. Novel methods for rapid freezing and thawing of foods - a review. J. Food Eng. 54,175-182.

Magnussen, O.M., Haugland, A., Hemmingsen, A.K.T., Johansen, S., Nordtvedt, T.S., 2008. Advances in superchilling of food - Process characteristics and product quality. Trends in Food Sci. Technol. 19, 418-424.

Marand, H.L., Stein, R.S., 1988. Isothermal crystallization of poly(vinylidene fluoride) in the presence of high static electric fields. I. Primary nucleation phenomenon. J. Polym. Sci, Part B: Polym. Phys. 26, 1361-1383.

Mazur, P., 1984. Freezing of living cells-mechanisms and implications. Am. J. Physiol. 247, C125-142.

Norio, O., Satoru, K., Inventors; ABI Limited, assignee. 2001 Jun 26. Super-quick freezing method and apparatus therefore. U.S. patent 6,250,087 B1.

Norton, T., Sun, D.W., 2008. Recent advances in the use of high pressure as an effective processing technique in the food industry. Food Bioprocess Tech. 1, 2-34.

Olmo, A., Baena, R., Risco, R., 2008. Use of droplet nucleation analyzer in the study of water freezing kinetics under the influence of ultrasound waves. Int. J. Refrig. 31, 262-269.

Orlowska, M., Havet, M., Le-Bail, A., 2009. Controlled ice nucleation under high voltage DC electrostatic field conditions. Food Res. Int. 42, 879-884.

Otero, L., Sanz, P.D., Guignon, B., Aparicio, C., 2009. Experimental determination of the amount of ice instantaneously formed in high-pressure shift freezing. J. Food Eng. 95, 670-676.

Petersen, A., Schneider, H., Rau, G., Glasmacher, B., 2006. A new approach for freezing of aqueous solutions under active control of the nucleation temperature. Cryobiology 53, 248-257.

Ricinschi, D., Okuyama, M., 2010. Study of partially-switched states of ferroelectrics in relation to the spatial inhomogeneity of their domain structure. J. Electroceram. 24, 33-38.

Saclier, M., Peczalski, R., Andrieu, J., 2010. Effect of ultrasonically induced nucleation on ice crystals' size and shape during freezing in vials. Chem. Eng. Sci. 65, 3064-3071.

Samaranayake, C.P., Sastry, S.K., Zhang, Q.H., 2005. Pulsed ohmic heating - a novel technique for minimization of electrochemical reactions during processing. J. Food Sci. 70, E460-465.

Schluter, O., Benet, G.U., Heinz, V., Knorr, D., 2004. Metastable states of water and ice during pressure-supported freezing of potato tissue. Biotechnol. Prog. 20, 799-810.

Shichiri, T., Araki, Y., 1986. Nucleation mechanism of ice crystals under electrical effect. J. Cryst. Growth 78, 502-508.

Shichiri, T., Nagata, T., 1981. Effect of electric currents on the nucleation of ice crystals in the melt. J. Cryst. Growth 54, 207-210.

Shim, J.Y., Lee, S.H., Jun, S., 2010. Modeling of ohmic heating patterns of multiphase food products using computational fluid dynamics codes. J. Food. Eng. 99, 136-141.

Simon, M.D., Heflinger, L.O., Geim, A.K., 2001. Diamagnetically stabilized magnet levitation. Am. J. Phys. 69, 702-713.

Sun, W., Xu, X., Sun, W., Ying, L., Xu, C. Effect of alternated electric field on the ice formation during freezing process of 0.9% K_2MnO_4 water. IEEE 8th International Conference on; 2006 June 26-30; Bali, Indonesia: Properties and applications of Dielectric Materials; c2006.

Sun, W., Xu, X., Zhang, H., Sun, W., Xu, C. The Mechanism Analysis of NaCl Solution Ice Formation Suppressed by Electric Field. IEEE 8th International Conference on;

2006 June 26-30; Bali, Indonesia: Properties and applications of Dielectric Materials; c2006.

Sun, W., Xu, X., Zhang, H., Xu, C., 2008. Effects of dipole polarization of water molecules on ice formation under an electrostatic field. Cryobiology 56, 93-99.

Toledo, E.J.L., Ramalho, T.C., Magriotis, Z.M., 2008. Influence of magnetic field on physical-chemical properties of the liquid water: Insights from experimental and theoretical models. J. Mol. Struct. 888, 409-415.

Ueno, S., Iwasaka, M., 1994. Parting of water by magnetic fields. IEEE Trans. Magn. 30, 4698-4700.

Vegiri, A., 2004. Dynamic response of liquid water to an external static electric field at T=250 K. J. Mol. Liq. 112, 107-116.

Woo, M.W., Mujumdar, A.S., 2010. Effects of electric and magnetic field on freezing and possible relevance in freeze drying. Dry Technol. 28, 433-443.

Zaritzky, N., 2011. Physical-chemical principles in freezing. in: Sun DW, (Eds.), Handbook of frozen food processing and packaging, 2nd ed.CRC Press, Boca Raton, Florida, pp. 3-38.

Zhang, G., Zhang, W., Dong, H., 2010. Magnetic freezing of confined water. J. Chem. Phys. 133, 134703.

Zhang, S., Wang, H., Chen, G., 2010. Addition of ice-nucleation active bacteria: *pseudomonas syringae* pv. *panici* on freezing of solid model food. LWT-Food Sci. Technol. 43, 1414-1418.

Zhu, S., Ramaswamy, H.S., Le-Bail, A., 2005. Ice-crystal formation in gelatin gel during pressure shift versus conventional freezing. J. Food. Eng. 66, 69-76.

CHAPTER 3

EFFECTS OF PULSED ELECTRIC FIELD (PEF) AND OSCILLATING MAGNETIC FIELD (OMF) COMBINATION TECHNOLOGY ON THE EXTENSION OF SUPERCOOLING ON CHICKEN BREASTS

3.1. Abstract

Extension of supercooling in a chicken breast was achieved using the combined pulsed electric field (PEF) and oscillating magnetic field (OMF). An accurate stair-shaped cooling rate control was implemented by combining of PEF codes with multiple duty cycles and OMF with a low frequency. The specifications of protocol are: (i) PEF with duty cycle sequence of 0.8, 0.5, and 0.2 were applied for 300 sec, 120 sec, and 90 sec, respectively and (ii) during PEF with duty cycle of 0.2, OMF with 1 Hz was applied to vibrate water molecules and inhibit sudden ice nucleation. At the freezer temperature of -7°C (± 0.5), temperature of chicken breast samples under PEF and OMF treatment decreased down to -6.5°C in a supercooling state during the whole testing period (approximately 12 hrs); while the control samples were fully frozen down to -6.5°C. The impacts of the supercooling on microstructure, drip loss, color, texture, pH and lipid oxidation were evaluated as compared with samples stored at refrigeration (4°C) and at freezing (-7°C). It was found that the PEF + OMF supercooling was highly effective in the maintenance of original meat qualities without significant physical damages or chemical changes. The supercoiling of meat samples using the developed PEF and OMF combination technique led to the advanced designing of innovative food freezers for long term preservation of ‘fresh-like’ foods at subzero temperature.

3.2. Introduction

With the large increase in demand for fresh meat quality, the meat processing has been developed to control and optimize the production in an economically favorable way. Based on the understandings of the significant factors on meat quality attributes, various methods for preservation are determined by demand changes regarding the various markets, local, regional and international and specifically the final use of meat.

Freezing technology has emerged and grown with long-term preservation without the major changes in the nutritional, chemical and physical aspects. However, freezing procedure and freezer storage inevitably influence meat quality attributes such as thawing loss, color and tenderness. The series of changes such as protein denaturation, lipid oxidation, and change in moisture take place in food products when subjected to excessively prolong frozen storage. The degree of structural damages by formation, growth, and distribution of ice crystals are directly related to those serial quality degradation of the frozen foods.

A large number of investigations have attempted to determine the mechanism of freezing in meat and the effect of freezing on meat quality with different animal meats, various sample dimensions, and different freezing and thawing methods (Ngapo et al., 1999; Molina-García et. al., 2004; Anese et. al., 2012). However, most of studies have been limited to technical issues due to a lack of fundamentals associated with physical properties and anomalies of water such as supercooling. To overcome these considerable issues, emerging freezing technologies have been developed based on water properties and most of them are aiming to induce the quick freezing of water by instant nucleation or ice crystal size controls by external stresses.

In present study, the potentials extension of the supercooling state in foods were investigated. By extension of supercooling state, it was expected that supercooled food products can be processed or consumed at freezing storage condition without quality deterioration by ice crystallization occurring even after long term. Previously, a number of studies have examined the supercooling phenomenon under different conditions and treatments such as pressure shift (Kalichevsky et al., 1995; Martino et al., 1998), irradiation of ultrasonic waves (Inada et al., 2001; Zhang et al., 2001), addition of polyvinyl alcohol (Kumano et al., 2011) and antifreeze proteins (Feeney and Yeh, 1998; Li and Lee, 1998). The effects of materials and shapes of the electrodes on supercooled solutions under electric field have also been investigated to characterize the degree of supercooling (Hozumi et al., 2003, 2005). Nevertheless, little work has been done on extension of supercooling in foods at freezing temperatures and periods of frozen storage. There are also limited numbers of studies available in the literature on the impact of supercooling on food quality traits.

To control the supercooling phenomenon, the combination of pulsed electric field (PEF) and oscillating magnetic field (OMF) were used in this study. As suggested in previous chapter, the electric field and magnetic field combination techniques are significantly influence the mobility of water molecules. With similar mechanisms but on different purpose, the PEF and OMF combination technique proposes that the stability of supercooling can be obtained using the control patterns with stair-shaped cooling rates by continuous reorientation and induced vibration motion of water molecules.

The innovative combination of PEF and OMF was tested for efficient extension of supercooling effect on frozen foods (i.e. chicken breasts), which is rarely achievable with

conventional methods. This study was conducted to examine the effect of the controlled supercooling on the structure and quality factors of chicken breasts, and compare with the control samples (refrigerated and frozen).

3.3. Materials and Methods

3.3.1. Meat preparation

Fresh chicken breast samples were trimmed of all visible connective tissue and excess fat and cut into 1.5” × 1.5” × 0.75” cubic blocks. All samples were weighed and wrapped in polyethylene (PE) film to avoid superficial dehydration before experiments.

3.3.2. Freezing equipment

A freezing system was designed and fabricated consisting of PEF and OMF modules and real-time temperature, current and voltage measurement units (Figure 3.1(a)). A freezing cube (1.5 × 1.5 × 1.5 $inch^3$), equipped with one pair of titanium plate electrodes in parallel, was placed on the top of the spacer block between the permanent magnet and electromagnet (Fig. 3.1(b)). For efficient cold air circulation, freezing cube was designed with plates with multiple holes. Magnetic forces were applied by a block of NdFeB permanent magnet (N52, DX88-N52, K & J Magnetics, Inc., Jamison, PA; size: 2 × 2 × 1 $inch^3$) and an electromagnet by alternating the charge and discharge to magnet wire (22 AWG, EIS, Inc., Atlanta, GA) coiled to iron core (VIMVAR, Ed Fagan, Inc., Franklin Lakes, NJ). The freezing unit fabricated with electric and magnetic fields was placed in the commercial chest freezer (FCM7SUWW, GE, Inc, Fairfield, CT).

(a)

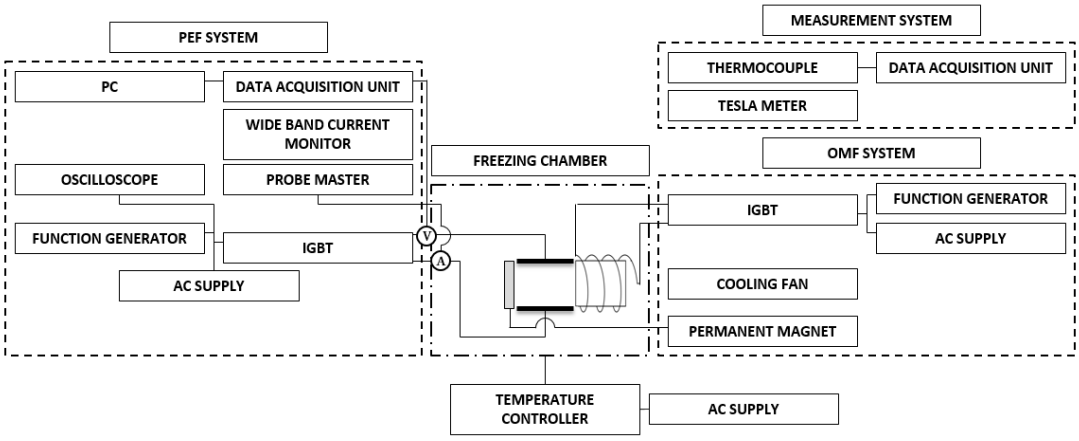

(b)

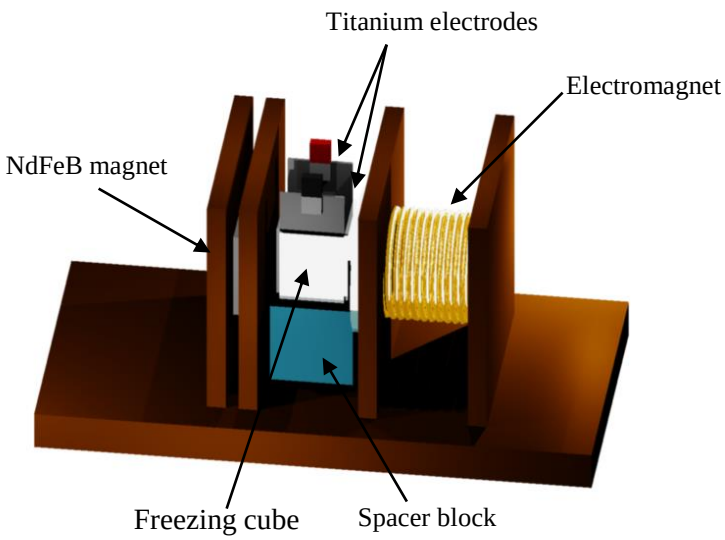

Figure 3.1. Schematic diagram of experimental apparatus. (a) Overall freezing system and (b) 3D view of freezing cube with PEF and OMF system.

The oscillating magnet field was generated by pulsed magnetic field with an intensity ranging from -150 to 150 mT. The applied voltage and pulse duty cycle was 25 V and 0.01, respectively and the applied frequency was as low as 1 Hz. In present study, the combined magnetic flux densities by permanent magnet and electromagnet were oscillated between 50 to 100 mT per second at the center of freezing cube. The pulsed

electric field was generated using an integrated-gate-bipolar-transistor (IGBT, IRAMX20UP60A, International Rectifier, El Segundo, CA) based power supply. Function generators (33220A, Agilent Technologies, Santa Clara, CA) were used to control the square wave forms with various duty cycles (D) and working frequencies. K-type thermocouple wire (K-type, PP-K-24S, Omega Engineering, Inc., Stamford, CT) and a data acquisition unit (DAQ, Agilent 39704A, Agilent Technologies, Inc., Palo Alto, CA) were used to monitor and collect the applied voltage and current, and temperature values of the sample and air in a freezer. The data were scanned and transmitted at the interval of 1 sec. The output signal was monitored in a digital oscilloscope (Model TDS2014; Tektronix, Beaverton, OR) and the magnetic flux densities between two different magnets were measured using a handheld teslameter (4060.50 AE Teslameter, Frederiksen, Inc., Ølgod, Denmark). Freezer temperatures were controlled using a digital temperature controller (A419, Johnson Controls, Inc., Milwaukee, WI).

3.3.3. Electrical conductivities of chicken breast during supercooling and freezing

A test cell was designed to measure electrical conductivities of food samples (Choi et al., 2011). To measure electrical conductivities of supercooled chicken breasts, samples were placed and contacted between two electrodes in a freezer operating at -7°C (± 0.5). Through the changes in electrical conductivities with temperature, the applied voltage and current were determined and tested for the desired cooling temperature profile. Acquired electrical conductivities of the samples were calculated by the following equation (Palaniappan and Sastry 1991):

$$\sigma = \frac{LI}{AV} \tag{3.1}$$

where L is the distance between two electrodes (m), A is the internal cross-sectional area (m^2), V is the applied voltage (V) and I is the measured electric current (A). From the obtained data, collected from 0^oC to temperature where begins to phase transition, the electrical conductivities of tested food materials were plotted against temperature and the temperature dependence of the measured electrical conductivity was depicted by a linear equation as given by:

$$\sigma = \sigma_{ref} + mT \tag{3.2}$$

3.3.4. Control of the cooling rate

In order to generate a stair-shaped cooling control logic, three different duty cycles, 0.2, 0.5 and 0.8 were used for the PEF treatment. The input voltage (5 $V_{p\text{-}p}$, peak-to-peak voltage) at the frequency of 20 kHz was determined to avoid electro-conducting heating even at the maximum duty cycle (0.8). The maximum electric current were estimated to 0.032A. To initiate the supercooling state in samples, 5 $V_{p\text{-}p}$ with duty cycle of 0.5 was applied to the samples until the electric current reached its minimum value in the supercooling state. From our preliminary tests, the use of 0.5 (on/off) duty ratio was closely associated with stabilization of the supercooling state and minimization of ice nucleation. In this first set of experiments, the effects of PEF with duty cycle sequences of 0.8, 0.5, and 0.2 on the cooling rate of chicken breasts were explored. The applied durations were 300 sec, 120 sec, and 90 sec, respectively. Duty cycle sequences were initiated after the electric current of chicken breast samples reached its minimum value for supercooling. The lower electric current showed the higher cooling rate and it caused sudden ice nucleation frequently. To suppress ice nucleation, the OMF was applied only with PEF duty cycle of

0.2. Using this protocols, the stair-shaped cooling rate controls were repeated until the temperature of samples reached to the freezer temperature, -7 ± 0.5°C. Four experiments were carried out to validate the reproducibility.

3.3.5. Microstructure analysis

The microstructures of chicken breast samples under different conditions (refrigeration at 4°C (control-), freezing at -7°C (control+), and supercooling by PEF and OMF combination at -7°C) were studied using an inverted microscope (Leica-DMIL, Wetzlar, Germany), and changes in cell morphology were evaluated. The dissected chicken samples were frozen in isopentane at −80°C, and series of 10μm-thick coronal sections generated with a Leica CM1900 cryostat (Leica Microsystems Buffalo Grove, IL). The structural changes by both intra- and extracellular ice crystals were estimated by measuring the likely cavity size located at the meat cross-sectional area in the equivalent circular diameter.

3.3.6. Drip loss

In this study, drip has been used to describe exudates both from frozen thawed meat (drip) and from refrigerated or supercooled meat (weep). The drip loss was measured according to the method previously described (Ngapo et al., 1999). Fresh meat samples were measured within 30 min after being cut from chicken breast chunk; drip loss of frozen samples were measured after thawing for 4 hours at 4°C. Five samples were used for each combination of freezing, thawing and storage. The samples were cut into six cubes of

approximately 0.5 inch length. Samples were suspended using nylon mesh and centrifuged at 40 × g for 90 min. Drip loss was measured as:

$$Drip\,loss(\%) = \frac{initial\,weight - final\,weight}{initial\,weight} \times 100 \tag{3.3}$$

3.3.7. Color measurement

To determine the effects of treatments had any negative effects on the appearance of chicken breasts, instrumental color analysis was conducted. The Hunter L^* (lightness), a^* (redness-greenness), and b^* (yellowness-blueness) values were measured using a color meter (ColorTec PCM, Clinton, NJ). The net color difference (ΔE) was calculated with the equation:

$$\Delta E = \sqrt{\left(L_2^* - L_1^*\right)^2 + \left(a_2^* - a_1^*\right)^2 + \left(b_2^* - b_1^*\right)^2} \tag{3.4}$$

where the subscripts 1 and 2 are referred to as color components before and after treatment, respectively.

3.3.8. Texture analysis

After cooking in a 70°C water bath for 30 min, texture was evaluated by shear force using a TA-XT2 texture analyzer (Stable Micro Systems, Godalming, UK) as described by Barbanti and Pasquini (2005) with a slight modification. The peak shear force (N) for 50% compression was measured using a 25 kg maximum cell load at a cross-head speed of 5 mm/s. Four measurements were performed on each sample.

3.3.9. pH measurement

The pH value of chicken meat was determined using 5 g samples, homogenized with 5 ml of water. The pH was measured using a digital pH-meter (Mettler Toledo, Columbus, OH) with direct insertion of the probe electrode after calibration. Measurements of pH were calculated from the average of four replicates.

3.3.10. Lipid oxidation measurement

Thiobarbituric acid reactive substances (TBARS) indicate the oxidative changes in muscle foods during storage. The amounts of TBARS in raw chicken breast samples were determined by using the procedure of McDonald and Hultin (1987). Sample (1 g) was weighed in plastic bags (ZipLoc, SC Johnson, USA) and homogenized with 10 ml of deionized water. Aliquot of the sample (1 ml) was added to 2 ml of trichloroacetic acid/thiobarbituric acid (TCA/TBA), consisting of 15% TCA (w/v) and 0.375% TBA (w/v) in 0.25 M HCl and 3 ml of 2% butylated hydroxytoluene (BHT) (w/v) prepared in ethanol and mixed thoroughly. The mixture was vortexed and incubated for 15 min in 90°C of water bath. The sample was cooled at room temperature for 10 min and centrifuged for 10 min at 1000 × g. The absorbance of the resulting supernatant solution was determined at 532 nm on a visible spectrophotometer (Thermo Scientific GENESYS20, Thermo Fisher Scientific, Inc., Rochester, NY). The TBARS values were calculated using a molar extinction coefficient of 1.56×10^5 $M^{-1}cm^{-1}$ and expressed as mg malondialdehyde (MDA) per kg of meat sample. For the measurement of lipid oxidation, four replicates were performed.

3.3.11. Statistical analysis

The results of this study are presented as the means, standard errors and analysis of variance (ANOVA) routine to test the significance of the dissimilarities between the means of testing parameters among the treatments ($P < 0.05$).

3.4. Results and Discussion

3.4.1. PEF and OMF combination

Electric current in supercooled raw chicken breasts during freezing process had kept changing. The decreasing temperatures of samples triggered a linear decrease in the amount of flows of electric charge (Fig. 3.2(a)). In addition, there was a deflection to the steep linear pattern around -3°C. Significant changes in the electric current values of chicken breast samples could be due to the initiated nucleation of water molecules inside chicken breast samples. These observations were confirmed by the changes of electrical conductivities as seen as a function of temperature. Before ice nucleation occurred, a linear correlation was observed ($R^2 = 0.969$, Fig. 3.2(b)). In contrast, no significant correlation between electrical conductivities and temperature was demonstrated after nucleation. The value of electric conductivities at 0°C was similar to the findings from Zell and others (Zell et al., 2009), 0.6 S/m. The abovementioned changes in electric current and electrical conductivity of chicken breast are substantially caused by ice formation and growth. It has been acknowledged as protonic defects of ice, cancelling the applied external electric field (Petrenko and Whitworth, 1999).

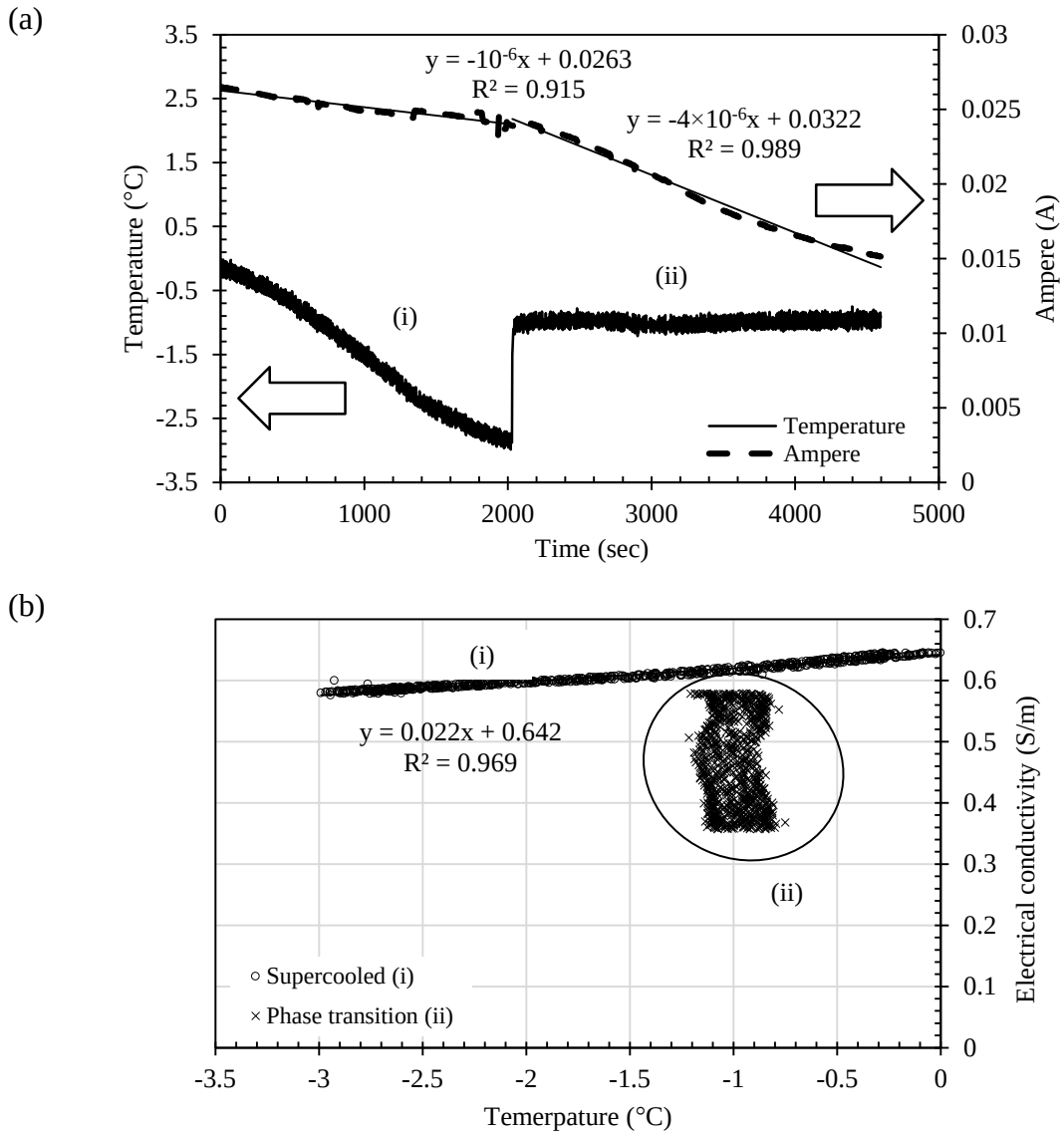

Figure 3.2. Electrical properties of chicken breasts during freezing process, consisting of (i) supercooling and (ii) phase transition. (a) Electric current changes over freezing process and (b) electrical conductivities of chicken breasts as a function of temperature. A circle indicates the changes of electric conductivities during (ii) phase transition.

The electrical properties of supercooling state in chicken samples are also given in Fig. 3.2. The supercooling was found in the temperature ranging from -1 to -3°C before

the sudden ice nucleation. The electrical conductivities of samples in suerpcooling state presented high linear correlation (R^2 =0.969) to be concluded as same linear function of temperature with those of unfrozen state samples. The decrease in electric conductivities in supercooling temperature range caused a decrease in electric current of samples and minimum electrical conductivity and electric current in supercooled chicken breasts were estimated to 0.580 S/m and 0.024 A, respectively, before nucleation occurred.

For full control of stable supercooling, the stair-shaped cooling rates was designed using PEF with the sequence of three duty cycles (Fig. 3.3(a)). Since the phase transition of water is highly correlated with its structure fluctuations and intermolecular networks (Moore and Molinero, 2009), the optimized controls for translational and orientational orders of supercooling state of water are required. The constant peak-to-peak voltages were applied to provide stable arrangement of water molecules periodically, it may assist the water to become a supercooling state. The PEF with duty cycles of 0.8, 0.5 and 0.2 was optimized to apply sequentially in different durations of 300, 120 and 90 seconds, respectively (t_1, t_2, and t_3, respectively, Fig. 3.3(a)). The different duty cycles and durations were aimed to generate the efficient cooling rate control in supercooling state. It was confirmed by the temperature profiles of the PEF treatment under each of the different duty cycle (Fig. 3.3(b)). It can be seen that maximum duty cycle of 0.8 resulted in the constant sample temperature. The decrease in duty cycles evoked an increase in cooling rates of chicken breast samples up to -0.12°C/min. The comprehension is that the duty cycle sequence bring about the modification of cooling rates to the stair-shaped temperature profile in supercooling state.

(a)

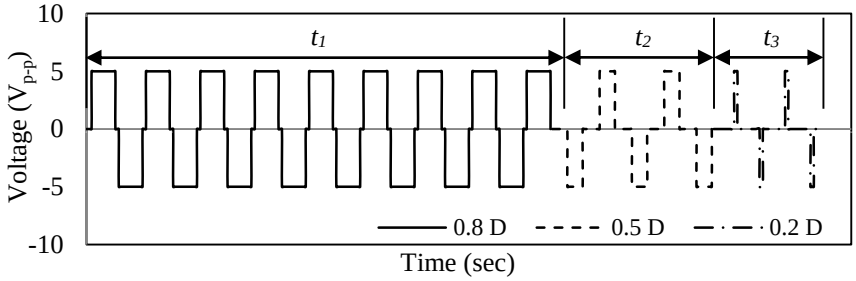

(b)

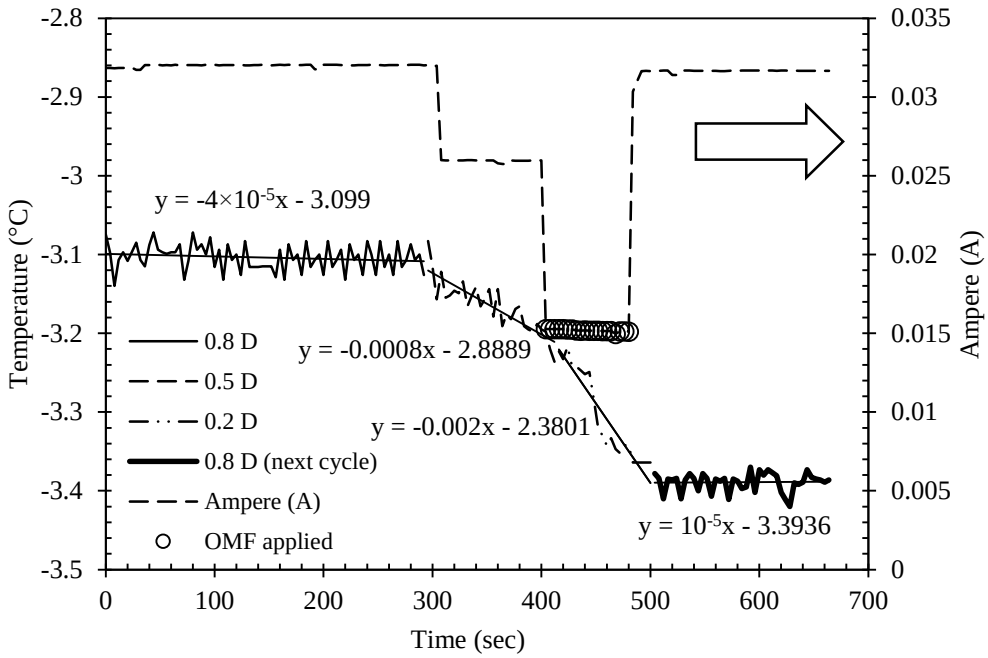

Figure 3.3. Modification of cooling rate of chicken breasts by strategically combined PEF and OMF treatments. (a) Square waveform pulsed electric field with duty cycle sequences of 0.8, 0.5 and 0.2 was applied for 300 sec, 120 sec, and 90 sec, respectively (t_1, t_2, and t_3, respectively) and (b) corresponding temperature profiles of chicken breasts with OMF treatment only when duty cycle of 0.2 was applied.

Despite the successful controls on stair-shaped cooling rate, the ice nucleation occurred instantly during the duty cycle of 0.2 were applied or when transited to duty cycle of 0.2 (data not shown). This is because of the weak electron distribution inside the sample,

leading to water molecules bringing back to native random states from their polarized alignments. This problem must be resolved before ice nucleation taking place, triggering the potential seed effects in nucleation on entire food matrix. In this experiment, the combined PEF and OMF treatments were applied to induce the vibrating motions of water molecules and promote the electron distributions inside chicken breasts. From others studies, the similar influences of magnetic fields on water molecules were reported; the pulsed magnet field can enhance the vibration motion (Iwasaka et al., 2011) and could be utilized for suppression of ice formation (Kiani and Sun, 2011). These proposed combination technologies successfully prevented the ice nucleation without any noticeable electrical interferences (Fig. 3.3(b)).

3.4.2. Effects of developed PEF and OMF combination on extension of supercooling

Fig. 3.4 shows the result of the temperatures as a function of freezing time under the combined PEF and OMF treatments using developed protocol. For comparison of the proposed PEF and OMF treatment protocol, the chicken breasts without any treatments were employed as control. It can be seen the same cooling rates on controls and the combined PEF and OMF treated samples before the controls became frozen. During this period, the combined PEF and OMF treatment was began to apply when electric current reached the minimum electric current in supercooling state (0.024 A). Therefore, it can be concluded that the developed PEF and OMF treatment are based on the interaction of water molecules rather than thermal effect.

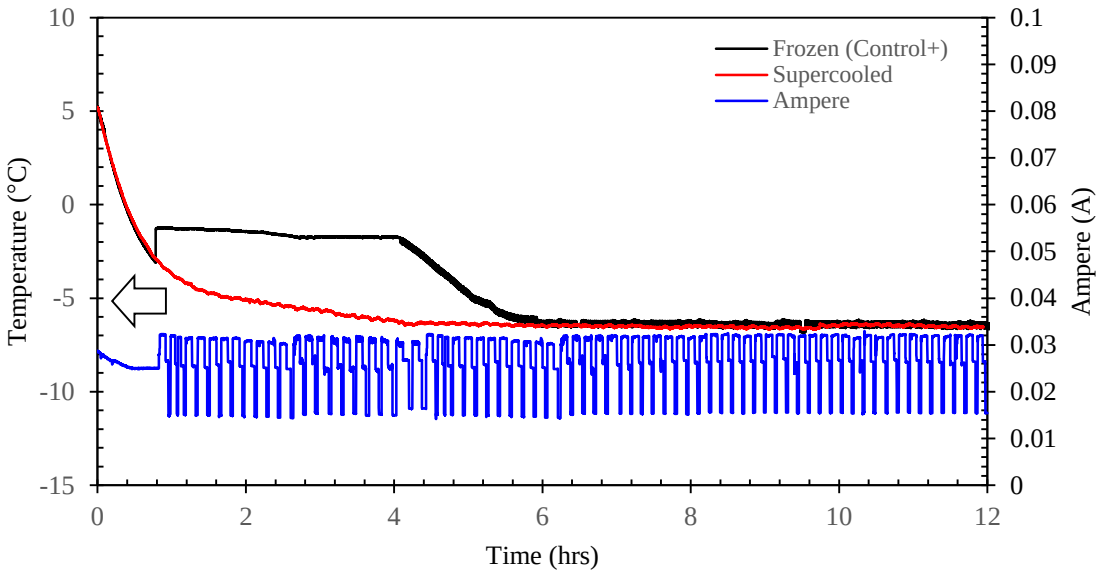

Figure 3.4. Temperature profiles of chicken breasts at -7 ± 0.5°C of ambient temperature. Control (black sold line) was fully frozen and reached to -6.5°C. On the other hand, samples with developed combined PEF and OMF treatments (red solid line) stayed in supercooling state during entire testing period.

The temperatures of PEF and OMF treated samples and controls were maintained at -6.5°C, close to the ambient temperature; The PEF and OMF treated samples remained as in a supercooling state (no ice nucleation), while the controls were fully frozen for 12 test hours. Since there is no freezing point on the chicken samples under PEF and OMF combination, the degree of supercooling of PEF and OMF treated chicken samples was estimated arbitrarily by the temperature difference between the freezer temperature and freezing point from controls. The mean degree of supercooling of chicken breasts under PEF and OMF treatment was 5.6 ± 0.2°C, as compared with 1.6 ± 1.4°C of controls. Besides, for reason that the supercooling state was maintained by PEF and OMF combination until

the end of experiments, the supercooling periods could not be quantified but extended furtherer than those of controls. In all cases, there was no sudden ice nucleation to the samples under the developed PEF and OMF treatment. Therefore, the control strategy using developed PEF and OMF combination was effective and applicable to maintain the supercooling state in chicken breast samples.

3.4.3. Effects of developed PEF and OMF combination on the microstructure of chicken breasts

The structures of sample tissues in supercooling state were illustrated by the optical microscopy and micrographs of representative images of chicken breasts after different treatments is shown in Figure 3.5. The micrograph images show that the refrigerated meats maintained their compact fiber tissues and no voids were observed between tissues. On the other hand, when the samples were frozen, the ice crystals were evident by some of voids and distortion of tissues. Even after short terms in frozen state, the fully frozen after the phase transition showed significant damages on meat samples. The equivalent circular diameters of cavities were estimated to 204 ± 70 μm. Note that the cavity sizes vary in whole cross-sectional area and a large number of freeze-cracks were proceeded. The micrographs corresponding to meat in supercooling (Fig. 3.5(c)) show no noticeable structural damage and cell disruption similar to the condition with refrigerated (unfrozen, Fig 3.5(a)). Thus, the cellular structure of supercooled chicken samples could be attributed to better and close to original cellular structure than frozen meat samples.

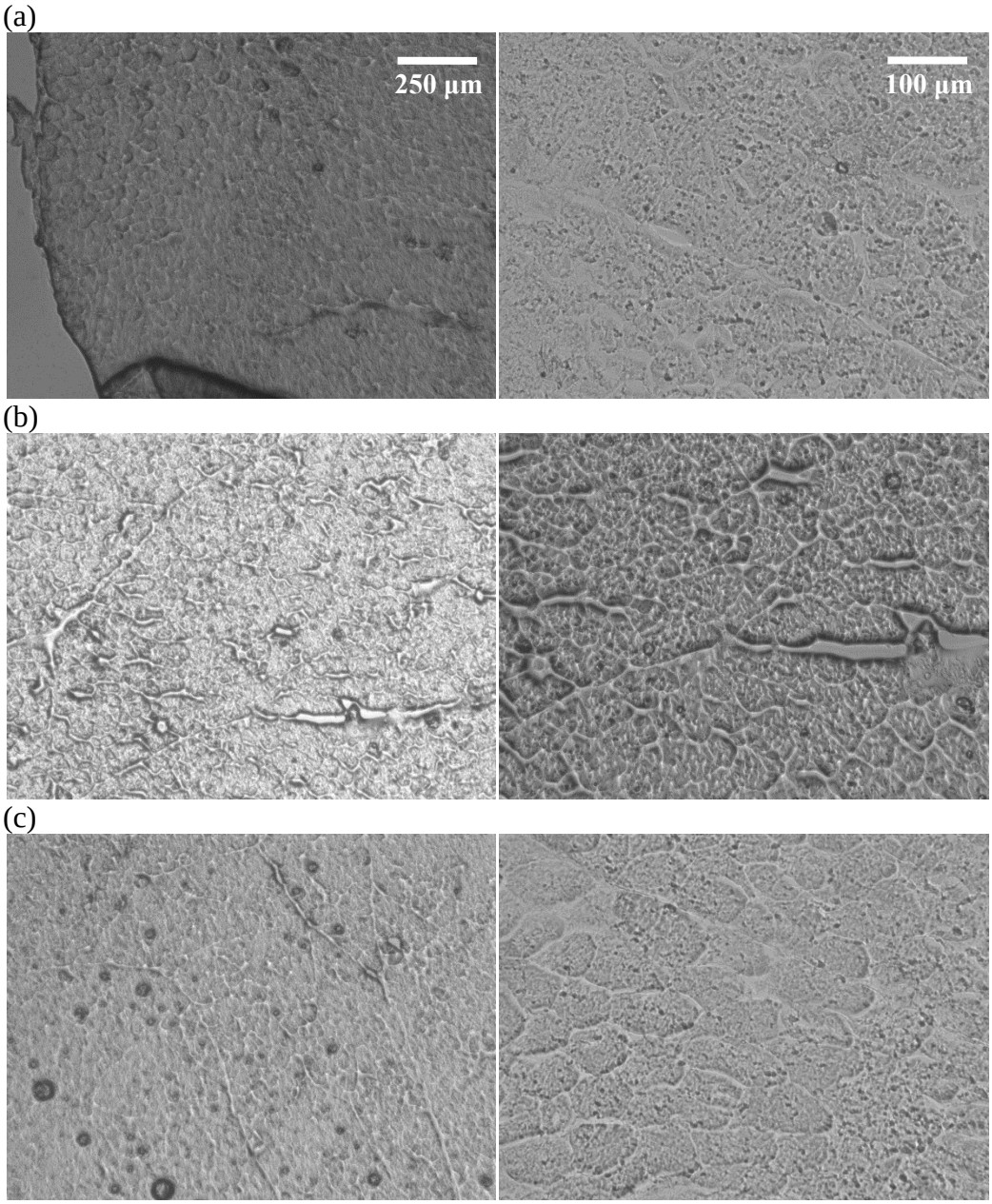

Figure 3.5. Micrographs of chicken breast samples under different condition. (a) Refrigerated at 4°C (control-), (b) frozen at -7°C (control+) and (c) supercooled by PEF+OMF at -7°C. The left and right side bars correspond to 250 µm and 100 µm, respectively.

3.4.4. Effects of PEF and OMF combination on the qualities of supercooled chicken breasts

Quality parameters, including drip loss, color, texture, pH and lipid oxidation, were measured to assess the quality changes on supercooled chicken breast samples. In comparison to the quality factors, the quality values of initial chicken breast samples at 4°C were considered as a respective controls. Table 1 shows that the quality parameter changes after different cold temperature storage conditions: fresh, refrigerated at 4°C for 12 hours, frozen and supercooled at -7°C for 12hours.

Regarding the drip losses, the values were not significantly different for fresh, refrigerated and supercooled chicken breasts. The chicken breasts frozen at -7 °C had only increase in drip loss which indicated myofibrillar shrinkage and muscle cell damages by the formation of ice crystals (Lee et al., 2008). As seen in the microstructure of breast after frozen storage (Fig. 3.5(b)), it was confirmed that the structural damage occurred in the muscle fibers caused to loss in water holding capacity, resulting in an increase of drip loss (Yoon, 2002; Lee et al., 2008). It has known that the loss in water holding capacity undergoes protein aggregation reactions which lead to toughening of the muscle (Mackie, 1993).

Compared to the shear force of corresponding control, the significant increase in tenderness was observed only in frozen chicken breasts ($P < 0.05$). The underlying mechanisms in the tenderisation are also derived from the breakdown of the muscle fibers and the loss of structural integrity caused by ice crystal formation. The formation of extracellular ice crystals disrupts the physical structure, largely breaking myofibrils apart

and resulting in tenderisation. Both refrigerated and supercooled chicken breasts were as tender as original samples ($P > 0.05$).

Table 3.1. Mean values (± S.D.) of physical and chemical changes over initial (at 4°C, Control), refrigerated (at 4°C for 12 hours, Control-), frozen (at -7°C for 12 hours and thawed at 4°C for 4 hours, respectively, Control+) and supercooled (at -7°C for 12 hours) chicken breast samples

Parameter	Initial	Refrigerated	Frozen	Supercooled
Drip loss (%)	0.83 ± 0.14^{a}	0.84 ± 0.05^{a}	1.74 ± 0.23^{b}	0.80 ± 0.13^{a}
Color change (ΔE)	N/A	0.35 ± 0.02^{a}	0.34 ± 0.01^{a}	0.33 ± 0.01^{a}
Texture (N)	$27.24 \pm 1.68^{a,b}$	27.17 ± 1.45^{a}	25.03 ± 2.24^{c}	27.80 ± 1.36^{b}
pH	6.40 ± 0.01^{a}	6.41 ± 0.01^{a}	6.40 ± 0.01^{a}	6.40 ± 0.01^{a}
TBARS (mg MDA/kg meat)	$0.26 \pm 0.03^{a,b}$	0.29 ± 0.02^{b}	0.27 ± 0.01^{a}	0.26 ± 0.02^{a}

In each rows, dissimilar small letters in each column indicate significant difference at 0.05 levels.

The measurements of TBARS in chicken samples demonstrated the amount of secondary oxidation product, malondialdehyde (MDA). The TBARS value of chicken breasts refrigerated was significantly higher than the chicken breasts in other conditions. The inhibition of TBARS was estimated at most 20% by freezing or supercooling as compared to refrigeration and it indicates that subzero temperature storages were effective

in reducing lipid oxidation of chicken breasts. The variation of the initial samples in the TBARS values might be derived from raw material variations or refrigeration conditions.

In both of pH and color difference measurements, there were no significant differences ($P > 0.05$) in all of values from different conditions. Although pH and color have known as significant effects on food qualities, there were no significant changes on a practical level in present study. It may be due to relatively short storage time projected in this study to other studies (Yu el al., 2005; Anang et al., 2010; Chun et al., 2010).

For the most part of quality tests, the supercooled chicken breast samples maintained the original fresh qualities. Overall, the findings of the current study demonstrate that the strategy of PEF and OMF combination for extension of supercooling state is applicable to maintain the original qualities while achieving satisfactory long term storage of raw chicken breasts. Furthermore, the optimized supercooling conditions under developed PEF and OMF combination technologies could deliver the premium food qualities to consumers.

3.5. Conclusion

The present study was conducted to test the PEF and OMF combination technique for effective extension of the supercooling status of food materials below the subzero temperature. The supercooling behavior of chicken breast samples was investigated and controlled using the developed PEF and OMF combination protocol. In addition, the results acquired from physicochemical tests showed that the supercooled chicken breasts maintained the original qualities without any quality deteriorations.

This study suggests the notable method for the extension of supercooling and benefits for supercooling preservation without physical or chemical damages from ice formation. Future studies may include designing of a commercial scale unit with larger sample scales that can guarantee premium quality of foods for the longer term preservation.

3.6. References

Anang, D.M., Rusul, G., Ling, F. H., Bhat, R., 2010. Inhibitory effects of lactic acid and lauricidin on spoilage organisms of chicken breast during storage at chilled temperature. Int. J. Food Microbiol. 144, 152-159.

Anese, M., Manzocco, L., Panozzo, A., Beraldo, P., Foschia, M., Nicoli, M.C., 2012. Effect of radiofrequency assisted freezing on meat microstructure and quality. Food Res. Int. 46, 50-54.

Barbanti, D., Pasquini, M., 2005. Influence of cooking conditions on cooking loss and tenderness of raw and marinated chicken breast meat. LWT-Food Sci. Technol. 38, 895-901.

Bédécarrats, J.P., David, T., Castaing-Lasvignottes, J., 2010. Ice slurry production using supercooling phenomenon. Int. J. Refrig. 33, 196-204.

Choi, W., Nguyen, L.T., Lee, S.H. and Jun, S., 2011. A Microwave and Ohmic combination heater for uniform heating of liquid–particle food mixtures. J. Food Sci. 76, 576-585.

Chun, H.H., Kim, J.Y., Lee, B.D., Yu, D.J., Song K.B., 2010. Effect of UV-C irradiation on the inactivation of inoculated pathogens and quality of chicken breasts during storage. Food Control 21, 276-280.

Dunn, A.S., Hemmingsen, A.K.T., Hauland, A., Rustad. T., 2008. Quality changes during superchilled storage of pork roast. LWT-Food Sci. Technol. 41, 2136-2143.

Feeney, R.E., Yeh, Y., 1998. Antifreeze proteins: current status and possible food uses. Trends in Food Sci. and Tech. 9, 102-106.

Hozumi, T., Saito, A., Okawa, S., Watanabe, K., 2003. Effects of electrode materials on freezing of supercooled water in electric freeze control. Int. J. Refrig. 26, 537-542.

Hozumi, T., Saito, A., Okawa, S., Eshita, Y., 2005. Effects of shapes of electrodes on freezing of supercooled water in electric freeze control. Int. J. Refrig. 28, 389-395.

Inada, T., Zhang, X., Yabe, A., Kozawa, Y., 2001. Active control of phase change from supercooled water to ice by ultrasonic vibration 1. Control of freezing temperature. Int. J. Mass Tran. 44, 4523-4531.

Iwasaka, M., Onishi, M., Kurita, S., Owada, N., 2011. Effects of pulsed magnetic fields on the light scattering property of the freezing process of aqueous solutions. J. Appl. Phys. 109, 07E320.

Kalichevsky, M.T., Knorr, D., Lillford, P.J., 1995. Potential food applications of high-pressure effects on ice-water Transitions. Trends Food Sci. Tech. 6, 253-259.

Kiani, H., Sun, D.W., 2011. Water crystallization and its importance to freezing of foods: A review. Trends Food Sci. Tech. 22, 407-429.

Kumano, H., Hirata, T., Takeda, S., Kudoh T., 2011. Quantitative evaluation of the effects of poly-vinyl alcohol on supercooling phenomena of water. Int. J. Refrig. 34, 1999-2006.

Lee, Y.S., Saha, A., Xiong, R., Owens, C.M., Meullent, J.F., 2008. Changes in broiler breast fillet tenderness, water-holding capacity, and color attributes during long-term frozen storage. J. Food Sci. 73, 162-168.

Li, J.K., Lee, T.C., 1998. Bacterial extracellular ice nucleator effects on freezing of foods. J. Food Sci. 63, 375-381.

Mackie, I.M., 1993. The effects of freezing on fresh proteins. Food Rev. Int. 9, 575-610.

Martino, M.N., Otero, L., Sanz, P.D., Zaritzky, N.E., 1998. Size and location of ice crystals in pork frozen by high-pressure assisted freezing as compared to classical methods. Meat Sci. 50, 303-313.

Martins, R.C., Lopes, V.V., 2007. Modelling supercooling in frozen strawberries: Experimental analysis, cellular automation and inverse problem methodology. J. Food. Eng. 80, 126-141.

McDonald, R.E., Hultin, H.O., 1987. Some characteristics of the enzymic lipid peroxidation system in the microsomal fraction of flounder skeletal muscle. J. Food Sci. 52, 15-27.

Miyawaki, O., Abet, T., Yano, T., 1989. A numerical model to describe freezing of foods when supercooling occurs. J. Food. Eng. 9, 143-151.

Molina-García, A.D., Otero, L., Martino, M.N., Zaritzky, N.E., Arabas, J., Szczepek, J., Sanz, P.D., 2004. Ice VI freezing of meat: supercooling and ultrastructural studies. Meat Sci. 66, 709-718.

Moore, E.B., Molinero, V., 2009. Growing correlation length in supercooled water. J. Chem. Phys. 130, 244505.

Ngapo, T.M., Babare, I.H., Reynolds, J., Mawson, R.F., 1999. Freezing and thawing rate effects on drip loss from samples of pork. Meat Sci. 53, 149-158.

Palaniappan, S., Sastry, S. 1991. Electrical conductivities of selected solid foods during ohmic heating. J. Food Process Eng. 14, 221-236.

Petrenko, V.F., Withworth, R.W., 1999. In: Physics of ice, Oxford University Press, New York. pp. 373.

Soyer, A., Özalp, B., Dalmış, Ü., Bilgin, V., 2010. Effects of freezing temperature and duration of frozen storage on lipid and protein oxidation in chicken meat. Food Chem. 1210, 1024-1030.

Tanaka, H., 2000. Simple physical model of liquid water. J. Chem. Phys. 112, 799–809.

Yoon, K.S., 2002. Texture and microstructure properties of frozen chicken breasts pretreated with salt and phosphate solutions. Poult. Sci. 81, 1910-1915.

Yu, L.H., Lee, E.S., Jeong, J.Y., Paik, H.D., Choi, J.H., Kim, C.J., 2005. Effects of thawing temperature on the physicochemical properties of pre-rigor frozen chicken breast and leg muscles. Meat Sci. 71, 375-382.

Zhang, X., Inada, T., Yabe, A., Lu, S.S., Kozawa, Y., 2001. Active control of phase change from supercooled water to ice by ultrasonic vibration 2. Generation of ice slurries and effect of bubble nuclei. Int. J. Mass Tran. 44, 4533-4539.

Zell, M., Lyng, J.G., Cronin, D.A., Morgan D.J., 2009. Ohmic heating of meats: Electrical conductivities of whole meats and processed meat ingredients. Meat Sci. 83, 563-570.